ISSN 2729-7640

ALFA ARCHITECTURE PAPERS
OF THE FACULTY OF ARCHITECTURE AND DESIGN STU
www.alfa.stuba.sk

2/2026 (Vol. 31)
DOI: 10.2478/alfa-2026-0010

Research article

Computational Fluid Dynamics-based simulation to analyse viral dispersion and spatial resilience in Tanzania

Benson Vedasto Karumuna[1]*

Buberwa Mukyamo Tibesigwa[2]

[1,2] Mbeya University of Science and Technology, College of Architecture and Construction Technology, Mbeya, Tanzania

***Corresponding author**
E-mail: karumunabenson@gmail.com

Article information
Sent: Apr 19, 2026
Accepted: May 26, 2026
Published: Jun 12, 2026

Abstract: An airborne transmission of COVID-19 in resource-constrained healthcare facilities, such as isolation centres in Tanzania, poses significant infection risks owing to insufficient ventilation. This study employs Computational Fluid Dynamics (CFD) to analyse airflow patterns within the 716 m^2 isolation centre of Shinyanga Regional Referral Hospital, aiming to identify high-risk regions and provide architectural remedies. A steady-state k-epsilon turbulence model with an 11×10^6 element mesh simulated both unoccupied and occupied conditions at breathing heights of 1.0 m and 1.7 m. Results demonstrate notable height-dependent airflow variations: the male ward maintained acceptable velocities (1.34–1.33 m/s) conducive to contaminant removal, but the triage and ante-lobby displayed insufficient inflow (0.08 and 0.031 m/s, respectively) when occupied. At a height of 1.0 m within the respiratory zone of bedridden patients, velocities diminished by up to 57% near bed railings, leading to the formation of stagnation pockets. Medical apparatus disrupted local airflow, diminishing velocities by 25-40% around ventilators. Turbulence kinetic energy was increased at 1.7 m (standing HCW level), indicating improved mixing. The airlock operated efficiently at 0.71–0.72 m/s. This work identifies airflow velocity and turbulence kinetic energy as verified surrogate indicators for the potential of contaminant dispersion, instead of employing direct virus dispersion modelling. Proposed resilience techniques include hybrid natural-mechanical ventilation, adaptable spatial reconfiguration, real-time indoor air quality monitoring, and sustained airflow maintenance (≥1.5 m/s at patients' bedsides). These findings provide a replicable, data-driven approach for improving airborne infection control in resource-limited hospital settings.

Keywords: COVID-19 isolation centre, Computational Fluid Dynamics (CFD), ventilation efficiency, airborne viral dispersion, infection control, spatial resilience,

1. Introduction

The prevention of the spread of infectious diseases that are transmitted through the air in healthcare settings has been a topic of concern concerning global health for a long time (Hiscott et al., 2020; Muralidar et al., 2020). When COVID-19 first appeared in Tanzania, it brought to light serious deficiencies in the spatial layout and ventilation efficiency of health institutions, particularly in isolation units that had been hastily established in response to the first crisis (Karumuna and Hao, 2024). There is still a lack of consistency in the actual execution of environmental control measures across resource-constrained contexts, even though infection prevention protocols have been previously incorporated into worldwide design standards in response to significant pandemics such as the Spanish flu.

Environmental controls are designed to reduce the number of microorganisms that are present on surfaces and in the air inside of buildings. This is accomplished primarily through the design of buildings, ventilation systems, and the regulation of airflow. The outbreak of COVID-19 in Tanzania revealed significant shortcomings in the spatial configuration and ventilation efficacy of healthcare facilities, especially in isolation units that were rapidly constructed in reaction to the first crisis (Karumuna and Hao, 2024). Despite the WHO's declaration of the cessation of the COVID-19 public health emergency in May 2023, the necessity for evidence-based design of isolation facilities persists. The ASHRAE Standard 241 (ASHRAE, 2024) on "Control of infectious aerosols" delineates new ventilation standards for healthcare environments, while the WHO 2025–2028 Global Health Strategy emphasises the importance of pandemic-resilient healthcare infrastructure. Resource-constrained environments such as Tanzania encounter specific obstacles in achieving these requirements, necessitating empirical analysis of current facilities to establish baseline performance and identify systems for enhancement.

Despite the incorporation of infection prevention protocols into global design standards in response to major pandemics like the Spanish Flu, there remains an inconsistency in the implementation of environmental control measures in resource-constrained settings. Therefore, looking into how

© 2026 Authors. This is an open access article licensed under the Creative Commons Attribution-International License (https://creativecommons.org/licenses/by/4.0/). Published by the Faculty of Architecture and Design, Slovak University of Technology in Bratislava, Slovakia

particulate matter spreads gives us a dependable but indirect way to tell how likely it is that viruses will spread. This research examines the developing architectural dialogue regarding the resilience of healthcare facilities (Capolongo et al., 2020; Şener et al., 2023). In contrast to engineering methods that prioritise mechanical system optimisation, architectural resilience examines how spatial configuration such as room geometry, adjacency connections, circulation pathways, and modular adaptability affect environmental performance. The COVID-19 pandemic illustrated that resilient hospitals must adapt and implement scientific airflow control (Ndayishimiye et al., 2022), yet the application of fluid dynamics to design principles is still inadequately examined in architectural literature, especially in sub-Saharan African contexts where resource limitations hinder fully engineered solutions.

Environmental controls are engineered to diminish the quantity of microorganisms present on surfaces and in the air within buildings. This is achieved mainly through the design of structures, ventilation systems, and the management of airflow. The WHO recommends the adoption of integrated infection control strategies to protect both patients and healthcare workers. To guarantee the containment and dilution of airborne pathogens, it is essential to employ suitable materials and techniques for airflow (WHO, 2009). Although international standards, such as those established by the ASHRAE (2020), prescribe a minimum of 6 air changes per hour (ACH) in non-critical patient rooms, Tanzanian healthcare institutions frequently fail to meet this recommendation due to limitations in both their infrastructure and processes. Operating rooms and isolation wards in developed settings have been the subject of a significant portion of the research that has been conducted recently. On the other hand, there have been fewer studies that have investigated emergency or isolation units in sub-Saharan Africa, particularly those that have utilised CFD to simulate the risk of respiratory transmission.

In the Shinyanga Region of Tanzania, a COVID-19 isolation centre is the focus of this research, which intends to investigate the patterns of airflow and the dispersion of airborne contaminants. Using CFD simulation techniques, this study examines the performance of existing ventilation setups, identifies regions within the facility that provide the largest risk of cross-infection, and proposes improvements to improve resilience and adaptability in the management of respiratory illness outbreaks. Additionally, it evaluates the effectiveness of existing ventilation setups and suggests adjustments to improve resilience and adaptability in the management of respiratory illness outbreaks.

2. Literature review

2.1. Using CFD to manage infection in healthcare facilities

The utilisation of CFD models for optimising indoor air quality has become the most effective technological tool for mitigating risks and hazards in the medical sector. In recent years, airborne transmission has been recognised as a major factor in healthcare-associated infections. Therefore, managing these illnesses and risks has emerged as a paramount responsibility in the healthcare sector to ensure the daily welfare of individuals. Considering these issues, many academics and medical professionals have developed models to assess the efficacy of hospital ventilation systems, concentrating on factors associated with airborne transmission (Agarwal et al., 2021; Li, 2023; Mata et al., 2022; Nair et al., 2022; Saeedi et al., 2023).

The dispersion and density of particulate matter, which transports viral aerosols, are closely associated with the transmission of airborne viruses. Although direct modelling of virus dispersion using particle tracking is beyond the scope of this investigation, airflow velocity and turbulence kinetic energy (TKE) are established as surrogate indicators for the potential of contaminant dispersion (Kaeophet et al., 2024; Liu et al., 2025). This method facilitates the identification of stagnation zones where aerosol accumulation may transpire, establishing a scientific basis for infection control measures. This research employs CFD modelling to simulate aerosol movement in enclosed isolation facilities, utilising velocity fields and TKE as proxies. This integration facilitates the identification of critical stagnation zones where viral particles may accumulate, providing a scientific foundation for infection control strategies and design enhancement in healthcare environments.

With an increase of evidence indicating the potential for airborne spread of the virus, containment centres for COVID-19 placed a greater emphasis on improving air quality. The foundation of this strategic approach was built upon the application of CFD. The utilisation of this robust computational instrument enabled a thorough understanding of airflow patterns and the spread of pathogens (CDC, 2024; Frank-Ito et al., 2016; Garcia et al., 2022). In recent years, CFD has grown widely used in a wide range of engineering fields to comprehend the flow of fluids better, the transfer of heat, and mass transport. CFD has been helpful in the healthcare industry in modelling airflows and tracing the spread of contaminants. Multiple factors, including airflow velocity, variations in temperature, and particle concentrations, can be considered in these simulations to mimic complicated scenarios (Peng et al., 2020; Runchal, 2024).

Over the past decade, CFD has become increasingly helpful in investigating hospital ventilation systems. A variety of ventilation systems, such as displacement ventilation, mixed ventilation, and individualised ventilation, have been evaluated using this method to foretell the distribution and concentration of particles, such as those small enough to be breathed; CFD models are frequently used in such research. In addition, CFD research has proven helpful in pinpointing "hot spots" wherein airborne pollutants may concentrate because of insufficient airflow. Results like these have a direct bearing on how we approach infection management in each setting, prompting us to rethink things like where we put air purifiers, how we regulate ventilation, and how we organise our daily routines (Lin et al., 2005a; Liu et al., 2019).

The application of CFD to healthcare has some restrictions, such as the necessity for model validation and computing limits. These challenges have been difficult to surmount, but significant developments in computing power and CFD programs are increasingly removing them. The significance of the airborne spread of infectious organisms within medical contexts was investigated by researchers. They emphasised ventilation systems, asserting that airborne disease transmission can be reduced through well-planned strategies. They modelled the spread of infections transmitted by air across the hospital and identified vulnerable areas using CFD (Mohamadi and Fazeli, 2022; Motamedi Zoka et al., 2021; Tsang et al., 2022).

2.2. Defining spatial resilience for healthcare facilities

According to Lin et al. (2025b) and the Harbin resilience in healthcare framework, spatial resilience in isolation facilities is defined by three quantifiable dimensions:

1. Transmissibility (flow efficiency): The capacity to sustain directional airflow from clean to polluted areas, measured by

maintaining a pressure differential of at least 2.5 Pa and velocity streamlines exhibiting a deflection of no more than 5°.

2. Diversity (spatial adaptability): The ability to reorganise spaces to accommodate evolving clinical requirements without significant infrastructural alterations, evaluated by the compatibility of modular partitions and the flexibility of utility systems. Recent research by Abbasi et al. (2024) on crisis engineering solutions for isolation zones illustrates that prefabricated components can be swiftly constructed while upholding infection control criteria.

3. Stability (performance consistency): Preservation of ventilation efficacy (≥1.5 m/s at the patient bedside) during fluctuating occupancy conditions, assessed by contrasting unoccupied and occupied velocity profiles.

This paradigm converts resilience from an abstract goal into measurable spatial performance standards. The Harbin study defines resilience in primary healthcare via "adaptive spatial design," facilitating a "dynamic balance in response to environmental effects" (Liu et al., 2025). This framework has been utilised in the construction of fever clinics in the post-pandemic period, generating definitive measures for spatial adaptability. It facilitates the evaluation of prospective consequences and contributes to the formulation of decisions, thereby providing a proactive strategy for infection control (Ahmadzadeh and Shams, 2022; Sheikhnejad et al., 2022).

Significant adjustments were implemented in containment centres because of incorporating CFD insights. The implementation of ventilation system enhancements has led to a heightened frequency of air changes, which has successfully mitigated the concentration of contaminated air. The implementation of HEPA filters in a strategic location contributed to an increased level of risk reduction, which was corroborated by CFD analyses. CFD has been utilised on a multitude of occasions to provide significant insights regarding the optimal positioning of healthcare personnel, patients, and apparatus to mitigate the potential for direct contact with aerosolised viral particles (Fadaei, 2021; Izadyar and Miller, 2022; Patel et al., 2022).

The potential future implications for infection control are contingent upon the knowledge acquired from the ongoing COVID-19 pandemic and the application of CFD methodologies, which can fundamentally transform the standards for designing healthcare infrastructure. It is anticipated that a greater understanding of airborne transmission and the importance of environmental factors will have a substantial influence on forthcoming protocols, consequently improving the degree of readiness for possible airborne pathogens (Beaussier et al., 2022; Gordon et al., 2021; Rayegan et al., 2023).

The application of CFD is vital to the optimisation of ventilation systems. By utilising sophisticated computational algorithms and methods, CFD permits an exhaustive examination and evaluation of ventilation patterns in a variety of spaces. CFD can simulate and analyse circulation patterns in confined spaces, as cited in Jeong et al. (2022) and Vuorinen et al. (2020). The utilisation of CFD techniques enables the identification of areas within rooms that are susceptible to air stagnation. Furthermore, CFD can be employed to forecast the path of aerosolised particles, thus assisting in the evaluation of dispersion characteristics (Kaeophet et al., 2024). Moreover, CFD can furnish valuable insights concerning optimal placements for ventilation and exhaust systems, thereby facilitating efficient ventilation. Engineers can evaluate and compare numerous CFD ventilation configurations via virtual experiments. It assists them in determining which of the competing designs to prevent the spread of disease is optimal (Alkhalaf et al., 2023; Arjmandi et al., 2022; Cho et al., 2022).

2.3. Design resilience and adaptability in health facilities

Resilience is a crucial aspect of any project that incorporates adaptive reuse. A facility that has design flexibility may be easily modified to meet new requirements without the need for major changes to the existing infrastructure. Health isolation facilities hold significantly more significance. The construction of these centres was completed rapidly, with a primary focus on addressing the COVID-19 pandemic. In the post-pandemic world, it is crucial for these establishments to be flexible and capable of accommodating a broader range of healthcare options. To achieve this objective, architects and designers should give priority to modular designs, movable partitions, and easily adaptable utility systems.

The COVID-19 pandemic brought to the forefront the critical requirement for healthcare infrastructure to adopt timely and adaptable strategies. Because of the increasing number of cases, many countries deemed it crucial to reevaluate traditional architectural and design methodologies, placing particular emphasis on the adoption of modular and flexible approaches customised for containment centres. The utilisation of CFD in these fields has demonstrated itself to be a paradigm shift, significantly enhancing the optimisation of ventilation and bolstering the level of safety within these design frameworks (Ndayishimiye et al., 2022; Pan and Zhang, 2022).

According to studies, a developing trend in healthcare is the creation of flexible and adaptable spaces. CFD was utilised in Li (2023) to simulate the effects of various partitions and configurations on airflow and infection risk. Their research demonstrated that CFD can assist architects in developing secure and adaptable designs. When employing modular designs, on-site assembly of prefabricated components is accomplished rapidly and without difficulty. It became imperative to promptly establish containment facilities in numerous areas, ranging from densely populated urban centres to remote rural regions, in response to the COVID-19 pandemic. To accommodate the requirements of individuals impacted by the ongoing pandemic, these units could be manufactured in an assortment of dimensions and equipped with a multitude of attributes. This is because their design possesses the essential qualities of scalability and efficacy (Gbadamosi et al., 2020; Li Chief Eng et al., 2022; Abbasi et al., 2024; Ren et al., 2021).

CFD is a computational instrument that is extensively utilised in the field of fluid mechanics to improve modular structures. Its primary purpose is to analyse and investigate fluid flow phenomena. It involves the examination of ventilation characteristics and patterns in a variety of constructed environments. The utilisation of CFD models in the examination of containment units for COVID-19 yielded significant findings concerning the possible spread of pathogens, the efficiency of ventilation systems, and the preservation of ideal temperature conditions. As previously stated, the analysis yielded significant findings that could be utilised to guide design choices, promote efficient airflow, and alleviate the hazards linked to airborne transmission (Katal et al., 2022; Li Chief Eng et al., 2022; Wang et al., 2022).

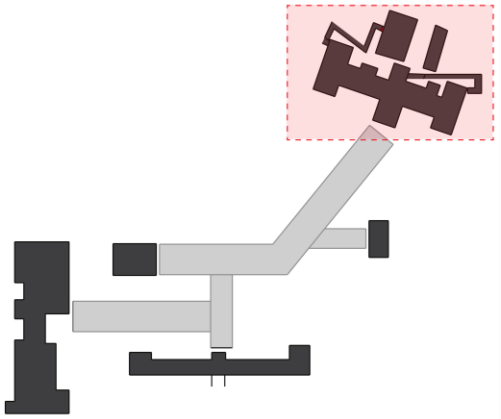
Furthermore, the epidemic has underscored the necessity for adaptability, which goes beyond the concept of modularity. As the scientific understanding of the virus advanced, commensurate adjustments were made to the specifications of con-

tainment centres. Moreover, authors note that there is evidence to suggest that units that were initially designed for brief periods of isolation may be reconfigured to accommodate intensive care environments or even extended durations. Consequently, adaptive designs were developed to accommodate current demands and demonstrate a proactive stance by predicting future necessities (Capolongo et al., 2020; Lam et al., 2022; Şener et al., 2023).

Moreover, research conducted by scholars Ding et al. (2022); Jeong et al. (2022), Tao et al. (2024) has emphasised the criticality of employing CFD to improve the flexibility of isolation centre designs considering the ongoing accumulation of data regarding the virus's transmission routes. Revisions to the design were necessitated by CFD findings, which guided modifications to the installation of barriers, adjustments to ventilation systems, and alterations to spatial configurations. The design modifications were substantiated by a robust scientific understanding foundation because of these revisions. In conclusion, the global pandemic has demonstrated the critical importance of adequate ventilation in patient chambers within hospitals. CFD techniques can be utilised to establish a proactive strategy for infection prevention. Using this information, it will be possible to modify several factors that protect public health by reducing the likelihood of transmission. Furthermore, complying with regulations is essential, but better ventilation systems are also crucial to any plan to promote public health.

3. Materials, data, and methods

3.1. Location and case description



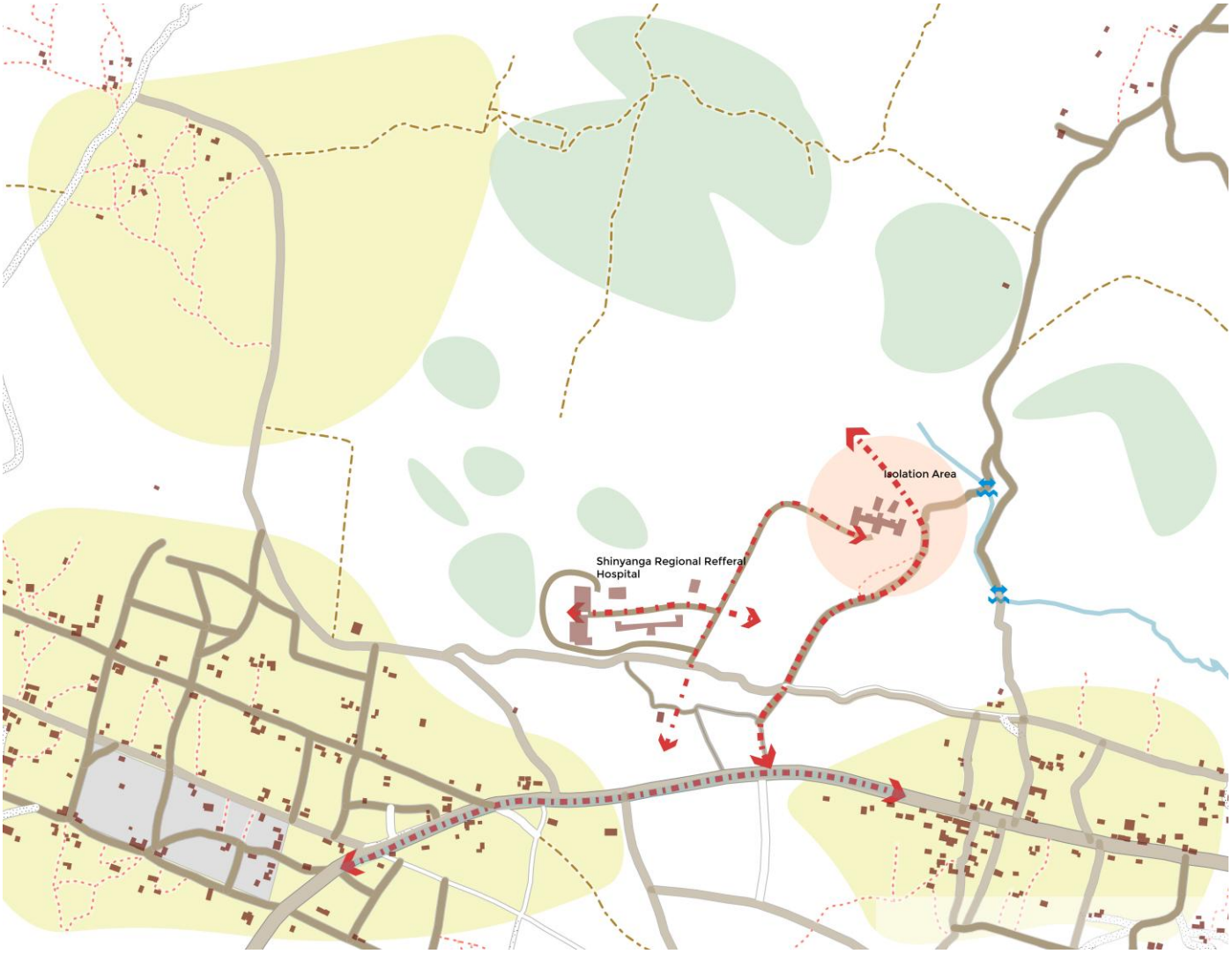


Fig. 1. Location of the SRRH: map (below) and isolation centre department (above). (Source: Authors, 2025)

Shinyanga Regional Referral Hospital (SRRH) is in the Shinyanga region as part of the region's referral hospital in Mwawaza (Tanzania), about 45 km from the Shinyanga town centre. While the hospital's neighbourhood seems to have

fewer residents, the containment centre is isolated from the main referral hospital buildings yet linked to them via a covered walkway (Fig. 1). SRRH, a prominent facility in Tanzania's lake zone that functioned as a front-line responder during the pandemic, is the subject of the case study, which focuses on the established COVID-19 isolation unit within the hospital. The unit, which was converted into a general hospital, is equipped with recovery bays, observation rooms, triage areas, waiting areas, and staff offices. A total floor area of the unit is roughly estimated at 716 m^2, and the spatial volume is approximately 2506 m^3 as seen in Fig. 2. Negative pressure was adjusted to −0.85 Pa in line with WHO (2021) recommendations for isolation wards, and the location of the SRRH isolation centre, as in Fig. 1, accurately represents this configuration, showing airflow velocity profiles within the space.

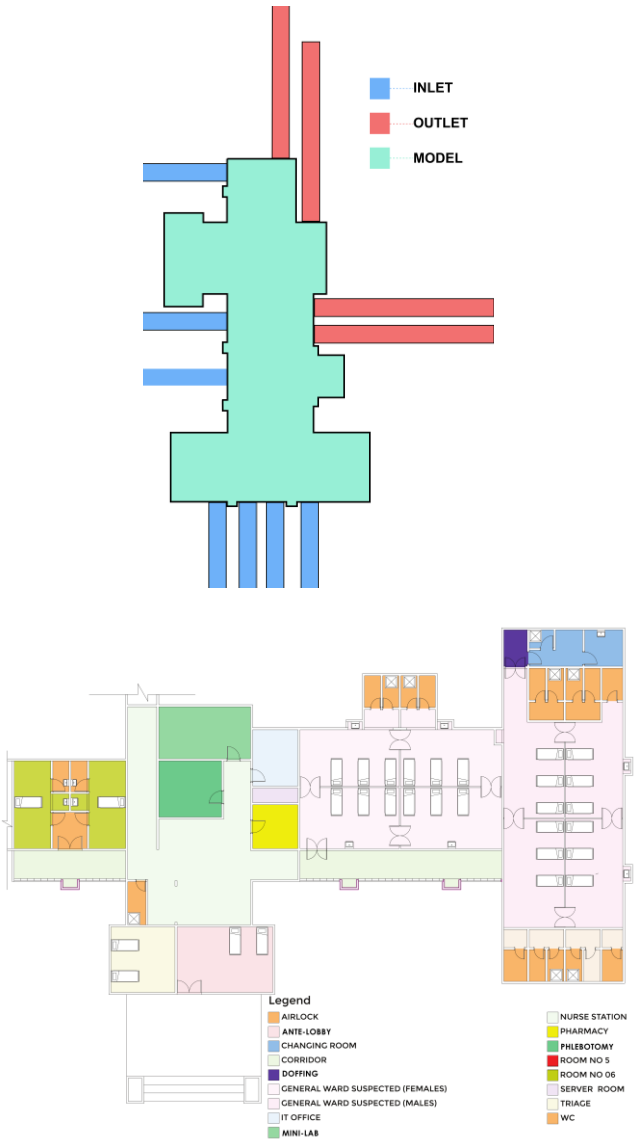


Fig. 2. The geometry of the SRRH – isolation centre: inlet & outlet air (above) and hospital layout (below). (Source: Authors, 2025)

The containment centre is a symmetrically designed building for containing COVID-19 victims, whereas the left wing of the building consists of wards for suspected cases, and confirmed cases are in the right wing. Generally, the building is designed to maximise isolation. It consists of six units, namely, triage rooms, wards, a laboratory and phlebotomy section; an intensive care unit; a staff building; and an end room, or mortuary. These units have been adopted for other uses currently, as the isolation centre now serves as an internal medicine department. The newly offered services include a physiotherapy department, optometry, and surgery.

Even though the building is mechanically ventilated, it does not have a fully integrated HVAC system that is ideal for the containment of airborne infections. The airflow system is comprised of air inlets and outlets that are installed on the ceiling and are positioned generally between 2.4 and 2.7 meters in height. The architectural layouts and ventilation parameters that were utilised in the simulation were derived from field evaluations and conversations with the engineering department of the hospital. To simulate the conditions that prevail during a pandemic, the CFD model incorporates furniture configurations and normal occupancy densities that are derived from observations and interviews with hospital staff. By following the protocols specified by the Tanzanian Ministry of Health, movement pathways for both patients and staff were constructed. These pathways were then verified using heat map modelling with the Autodesk Revit 2024 (Revit 24) program. To model human presence, modified cuboid geometries with an average height of 1.7 meters were utilised. These geometries were designed to approximate real-world interaction locations.

3.2. Boundary conditions

The air was modelled to replicate standard interior conditions in Shinyanga, with a temperature of 25°C and a relative humidity between 30 and 60 percent. The subsequent boundary conditions were implemented. Velocity inlets were set with a default turbulence intensity of 5%, while pressure outputs were maintained at 0 Pa gauge. Two primary scenarios were examined: one depicting an empty condition to establish baseline airflow dynamics and the other illustrating an occupied condition with furniture and simulated human presence. Both scenarios were predicated on traditional distributions of patients and personnel.

3.3. CFD setup

To analyse the behaviour of the airflow within the COVID-19 isolation centre, the simulation was carried out on Computational Fluid Dynamics 2024 (CFD 24); microclimate analysis was performed by Autodesk Forma 2023, and Andrew-mesh 3D sun path performed the sun path study. The two-dimensional technical drawings that were provided by the engineering department of the hospital were used to create a digital reconstruction of the building's internal geometry. To create the fluid domain suitable for airflow modelling, solid components were eliminated using Boolean subtraction. A computational mesh consisting of about 11×10^6 elements was developed to guarantee the independence of the mesh shown in Fig. 3. The resolution was optimised based on airflow velocity profiles at 1.7 meters and distributed according to the density shown in Fig. 4, which corresponds to the average breathing height of healthcare workers and patients. In the simulation, a steady-state approach was taken, and the conventional k-epsilon turbulence model was utilised.

To simulate the typical indoor circumstances in Shinyanga, the air was modelled at a temperature of 25°C and a relative humidity that ranged from 30 to 60 percent. To simulate the effects of suction within the ventilation system, velocity inlets were configured with a default turbulence intensity of 5%, and pressure outputs were fixed at 0.85 Pa, as can be seen in Tab. 1. There were two principal scenarios that were analysed: one represented an unoccupied state to establish baseline airflow behaviour, and the other represented an occupied state that featured furniture and mimicked human presence. Both sce-

narios were based on conventional patient and staff distribution patterns. To determine the speed at which particles travel, performance metrics were utilised. These metrics included velocity magnitude, which was measured in metres per second; turbulence kinetic energy (k), which was used to assess the levels of air mixing and aerosol dispersion; and airflow streamlines, which were utilised to track potential transmission routes between functional regions of the isolation centre. In addition, the quality of the study in Tab. 1 is within the boundaries of the conventional standard values for similar study cases (Alrebi et al., 2022; Jiru and Bitsuamlak, 2010). After the mesh has been created, it has been exported to the CFX PRE to define the required configuration that corresponds to the study.

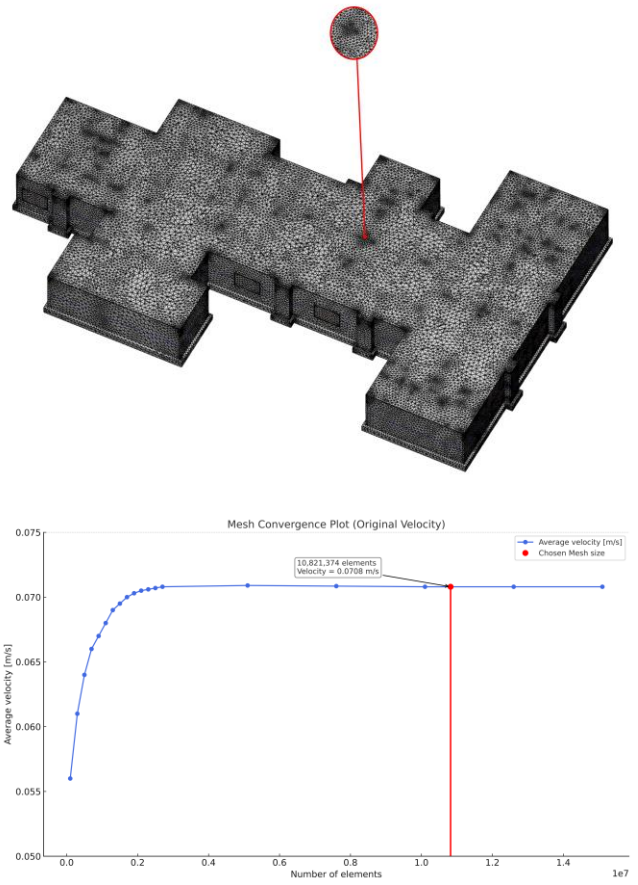


Fig. 3. Model CFX mesh (above) and sensitivity analyses of the mesh on average velocity (below). (Source: Authors, 2025)

For the CFD simulation of the isolation room, a computational mesh was generated. The core mesh sizing parameters are summarized in Tab. 2 with a maximum element size of 109 mm, a growth rate of 1.33, and a total of about 10.82 million elements. Geometric details were resolved with a defeature size of 0.6 mm. Tab. 3 summarizes the settings for curvature and inflation layer, where the curvature normal angle was set to 20° and the minimum curvature size was 1.2 mm. 4 inflation layers were generated with a transition ratio of 0.81 to better capture the velocity gradients near the wall. The maximum skewness was 0.85.

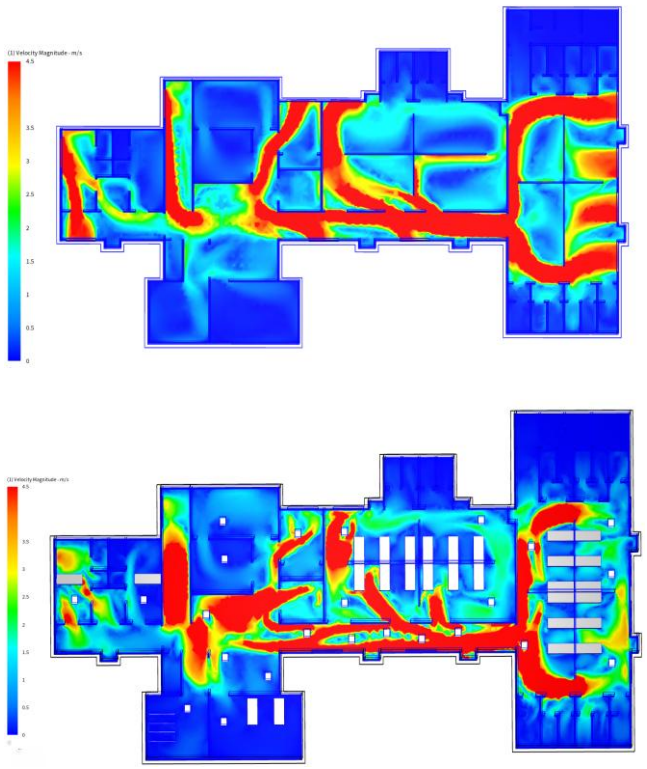


Fig. 4. Velocity magnitude: (left) Movement heatmap without people & furniture and (right) Furniture arrangement with people. (Source: Authors, 2025)

Tab. 1. CFD boundary conditions. (Source: Authors, 2025)

Parameter	Value	Justification
Negative pressure Differential	-0.85 Pa (relative to adjacent spaces)	WHO (2021) isolation ward standard
Pressure outlets	0 Pa (gauge, atmospheric reference)	Standard practice for indoor airflow
Inlet velocity (supply diffusers)	0.5-2.5 m/s (zone-dependent)	Field measurements at SRRH
Turbulence intensity	5%	Default for indoor airflow (ASHRAE, 2023)
Turbulence model	Standard k-epsilon	Widely validated for indoor airflow
Air temperature	25°C ± 1°C	Shinyanga typical indoor conditions
Relative humidity	30-60%	Seasonal variation

Tab. 2. Mesh properties. (Source: Authors, 2025)

Property	Value
Elements' maximum size (mm)	109
Number of elements	10.82 x 106
Growth rate	1.33
Defeature size (mm)	0.6

Tab. 3. Mesh properties. (Source: Authors, 2025)

Property	Value
Curvature minimum size (mm)	1.2
Curvature normal angle (degree)	20
Skewness	0.85
Inflation transition ratio	0.81
Inflation number of layers	4

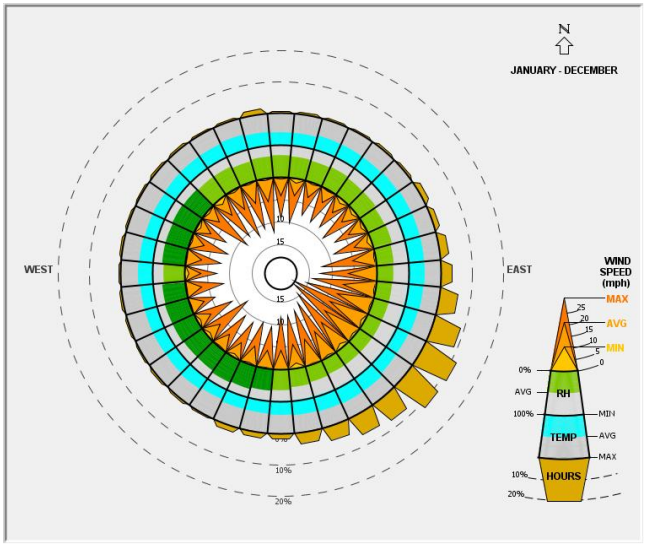
4. Results

4.1. Microclimate conditions

The SRRH isolation building faces a tropical savanna milieu with substantial seasonal swings that raise dust dangers, from hot, humid conditions (Nov–Apr: 32°C/85% relative humidity - RH) that promote virus persistence to dry seasons (May–Oct: 30% RH). Critical microclimate issues include urban heat island effects (2–3°C higher), seasonal wind pattern perturbation, and 90% RH increases after rain. Implementations can address these while optimising infection management: hybrid cooling with night-flush ventilation (8–10°C diurnal swings) and desiccant-assisted HVAC in humid months; bioclimatic envelope designs with phase-change roof panels (28°C melting point). Features include functional louvers (40-60% openness) for temperature regulation, CFD-optimised windbreak position (NE side), UVGI-enhanced exhaust (50 J/m^2 dosage), and microclimate awareness.

4.2. Wind

The COVID-19 isolation centre at SRRH offers good wind for natural ventilation, affecting airflow and infection control. The wind rise and flow field simulation suggests 54% southeast (135°) wind flow at the site. This trend suggests architectural openings and ventilation systems for capturing airflow from this direction. The simulation shows that airflow is concentrated over longer facades, and wind shadows form behind buildings, notably on the northwest side, restricting natural ventilation.



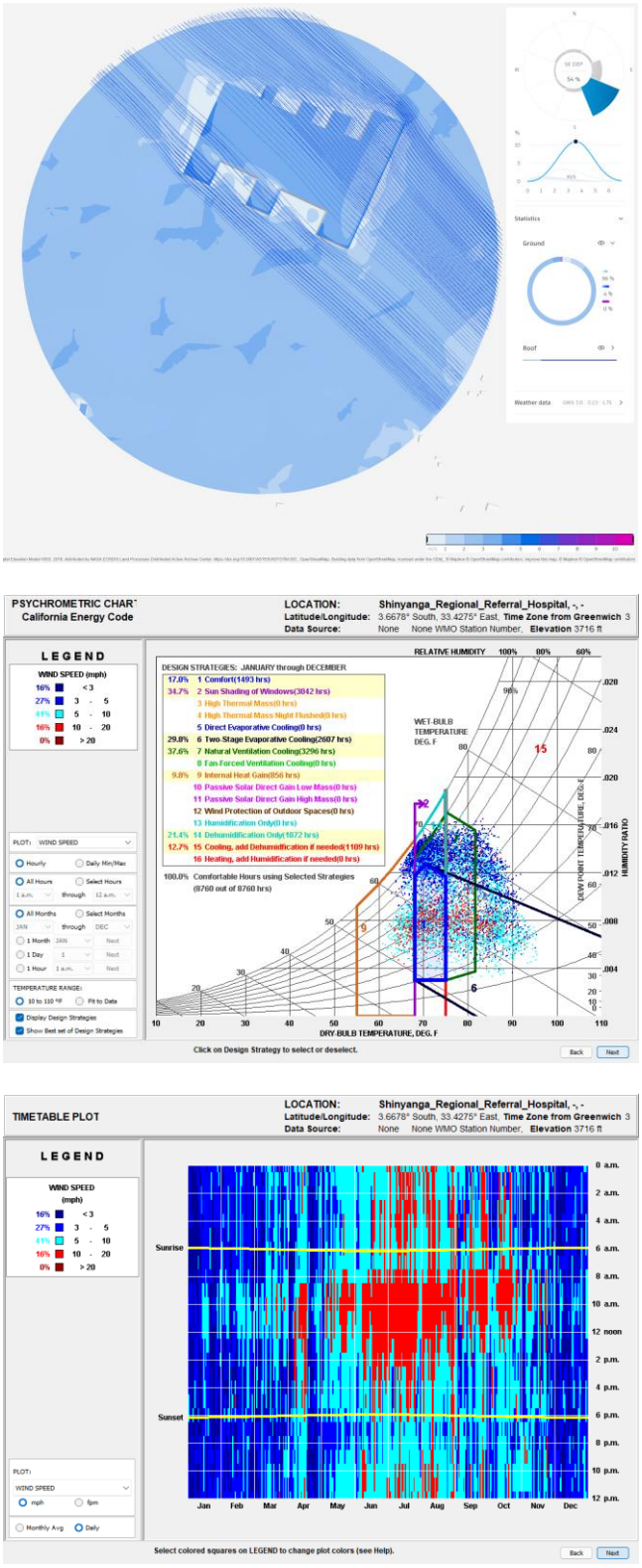


Fig. 5. (left) Jan–Dec windwheel flow pattern; (from top to bottom) Outdoor wind; Psychrometric chat wind speed; Timetable plot wind speed. (Source: Authors, 2025)

3D charts demonstrate that 90% of Fig. 5's wind speeds are 3 to 10 mph, increasing at 13.14 mph between midday and early evening from March to August. This stability in medium winds optimises daytime passive ventilation. Mechanical ventilation may be essential in the mornings and evenings due to low wind activity. The power density chart shows that the 10% windiest areas have a mean power density of 27 W/m^2, which is suitable for passive ventilation but not for ideal wind energy generation. This data encourages strategic facility orientation,

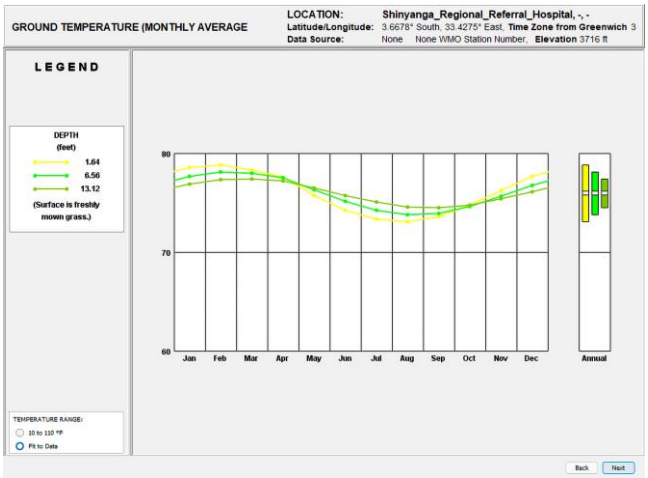
hybrid ventilation systems, and design layout that improves air circulation in high-occupancy and medical areas and minimises low-ventilation regions through architecture or landscape.

The SRRH COVID-19 isolation facility possesses favourable wind conditions for natural ventilation, influencing airflow and infection management. The wind rise and flow field simulation indicates a 54% southeast (135°) wind flow at the location. This tendency reveals openings in the architectural design and ventilation systems for the collection of airflow from this direction. The modelling findings indicate that airflow is directed over extended facades, creating wind shadows behind the buildings, particularly on the northwest side, which restricts natural ventilation. 3D charts indicate that wind speeds in Figure 5 predominantly range from 1.34 to 4.47 m/s (3–10 mph) at a 90% frequency, with a peak of 5.87 m/s (13.14 mph) occurring from midday to early evening between March and August. The mean power density in the top 10% of windiest locations is 27 W/m^2, which is enough for passive ventilation but suboptimal for wind energy production. The mean power density in the top 10% of windiest locations is 27 W/m^2, which is enough for passive ventilation but suboptimal for wind energy production, as depicted in Tab. 4.

Tab. 4. Basic data points recap. (Source: Authors, 2025)

Metric	Value
Dominant wind path	135° (SE) – 54%
Max wind speed	13.14 mph with approx. 5.87 m/s
Popular speed range	3–10 mph for 90% frequency
Calm wind environments (<3 mph)	2%
Mean power density (10% Windiest)	27 W/m^2
Peak ventilation time	Noon–6 PM from Feb–Oct

4.3. Temperature



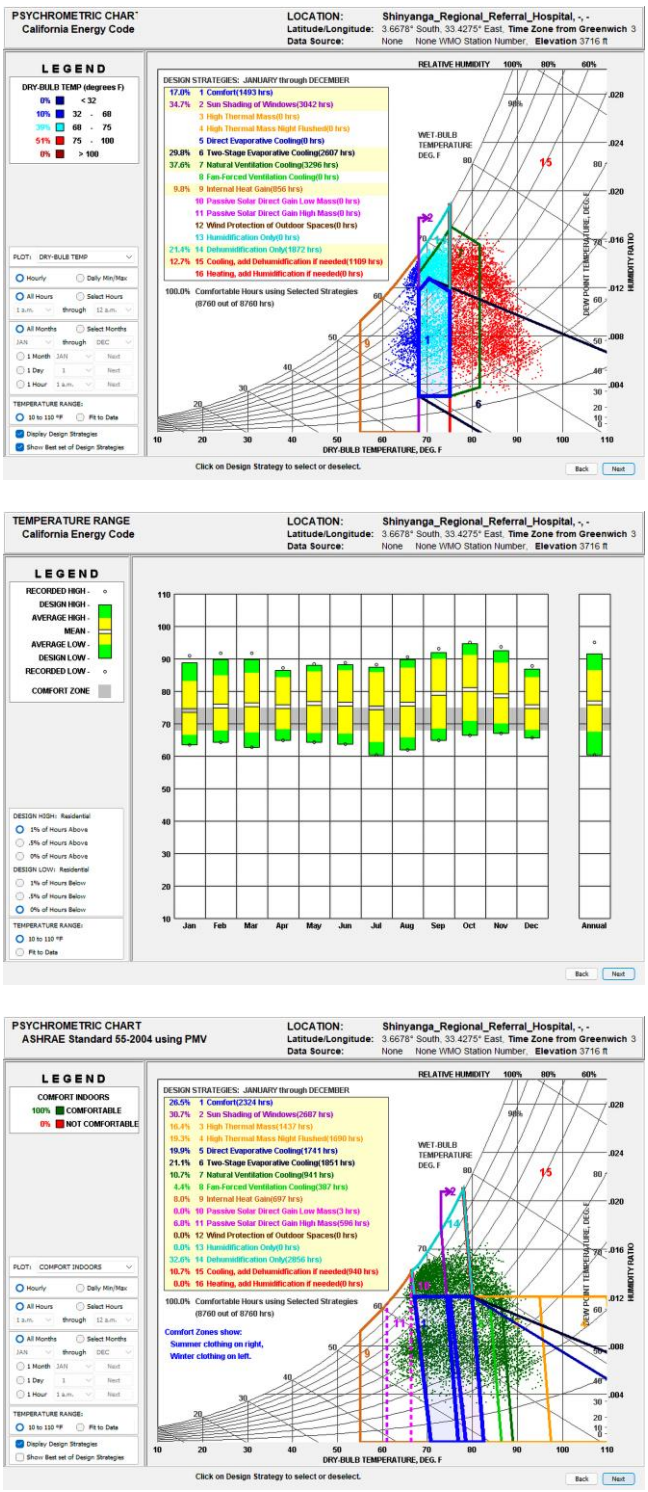


Fig. 6. Temperature and climatic conditions of SRRH (left) Monthly ground temperature; Psychrometric chart dry-bulb temperature; (right) Monthly temperature range; and Psychrometric chart comfort indoors. (Source: Authors, 2025)

In Fig. 6, Shinyanga, Tanzania's ground and wet bulb temperatures revealed seasonal variations affecting thermal comfort, humidity, and viral persistence in COVID-19 isolation centres. Ground temperature ranges from 21°C in cooler months to 32°C in warmer months. Deeper stable thermal mass layers (2–4 meters) cool passively. Wet bulb temperatures above 27°C in humid months can produce heat stress and increase virus survival risks, compared to 20°C in dry seasons. Earth beaming and thermal mass incorporation to stabilise indoor temperatures; a hybrid HVAC system with dehumidifiers in humid months and evaporative coolers in dry seasons; stack

ventilation in hot months and HEPA-filtered mechanical ventilation in stagnant, humid months; and CFD modelling of worst-case scenarios are recommended to improve infection control and airflow resilience. These activities ensure energy-efficient and climate-adaptive spatial resistance against viral propagation.

4.4. Relative humidity

In Fig. 7, the psychrometric study of Shinyanga shows that wet season from November to April, 60–80% RH, and dry season from May to October, 30–50% RH, affect viral transmission and ventilation efficiency. Dry bulb temperatures above 85°F and relative humidity over 60% (summer maximum) enhance viral survival and threaten thermal comfort, requiring dehumidification and air changes (8–12 ACH). Evaporative cooling works best in dry conditions; however, dust may be conveyed. These issues have solutions: desiccant dehumidifiers, mechanical ventilation zoning with HEPA/UV for wards during dangerous times and natural cross-ventilation in other areas during nice weather; smart humidity buffers that use hygroscopic interior decoration to stabilise relative humidity between 40 and 60%, and CFD-optimised airflow routes that take seasonal psychrometric variations into account, especially for model, are used in HVAC systems that work in both humid and dry periods. These stages require 25–40% less energy than standard approaches and produce climate-resilient infection control. In Fig. 8 the monthly precipitable water values peak at approximately 62 mm during the summer months (Jun–Aug) and reach a nadir of about 16 mm in the winter (Jan–Feb). The yearly variation in ambient moisture levels affects latent cooling requirements and humidity management in the isolation facility.

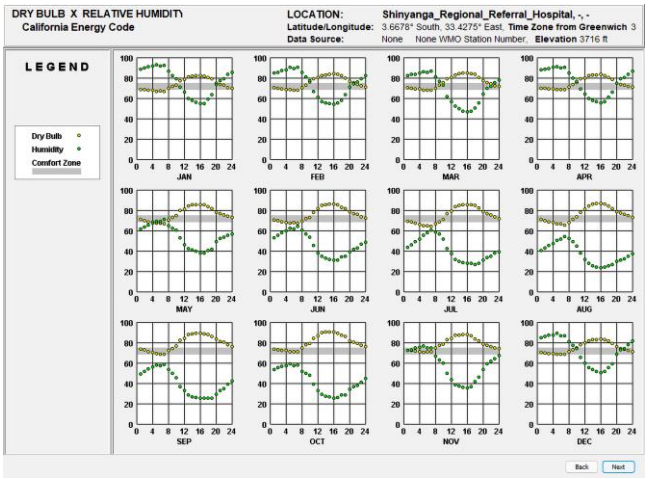


Fig. 7. Monthly relative humidity. (Source: Authors, 2025)

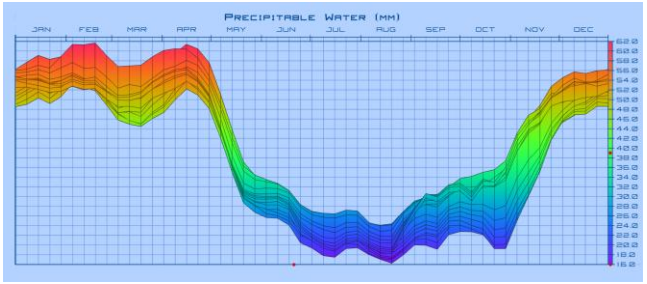


Fig. 8. Annual precipitation rate. (Source: Authors, 2025)

4.5. Solar radiation

Shinyanga, Tanzania's diffuse solar radiation analysis shows critical seasonal oscillations in scattered sunshine that affect indoor airflow, thermal comfort, and direct sunlight in a COVID-19 isolation centre. In Fig. 9, more diffuse radiation (perhaps during wet seasons) shows decreased direct UV disinfection and reduced thermal-driven ventilation, requiring artificial airflow support. Lower diffuse periods (dry seasons) provide more sunlight for natural UV sterilisation but risk overheating. Adaptive glazing to balance daylight and heat gain, hybrid ventilation systems like HEPA for humid months and air flow for dry seasons, UV-reflective surfaces for passive disinfection, and CFD modelling of seasonal radiation patterns to customise airflow rates are design strategies. This ensures climate-resilient infection management by harnessing solar dynamics to decrease viral dispersion and maintain energy economy.

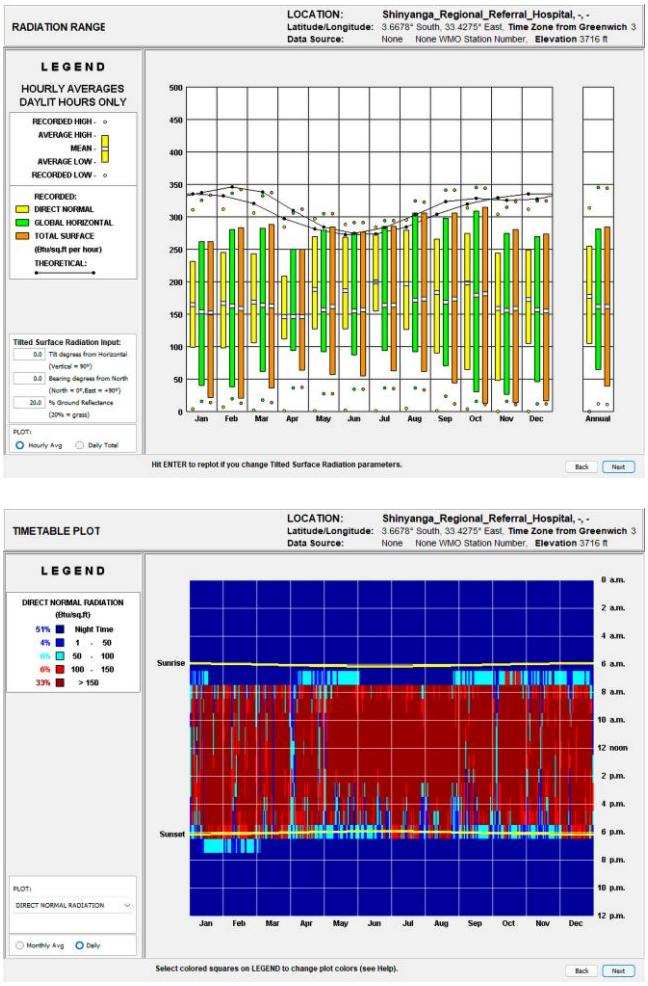


Fig. 9. Solar radiation (top) Annual radiation range; and (bottom) Timetable for annual radiation rate. (Source: Authors, 2025)

4.6. Sun path

The solar path analysis for Shinyanga, Tanzania, presents several useful insights on how solar altitude, daylight period, and sun position alter throughout the year. These factors affect natural ventilation, thermal comfort, and UV exposure, which are crucial for COVID-19 isolation centre infection management. Here is a full study of how the data relate to CFD-based viral dispersion and geographic resilience research. In Fig. 10, SRRH solar path analysis shows seasonal fluctuations in solar altitude (48.030 in June to 75.97° in March) and daylight length (11:55 a.m. to 12:20 p.m.) in a COVID-19 isolation

centre. Variations affect natural ventilation, thermal comfort, and UV exposure. Higher sun angles, like the March equinox, may increase heat absorption and UV disinfection.

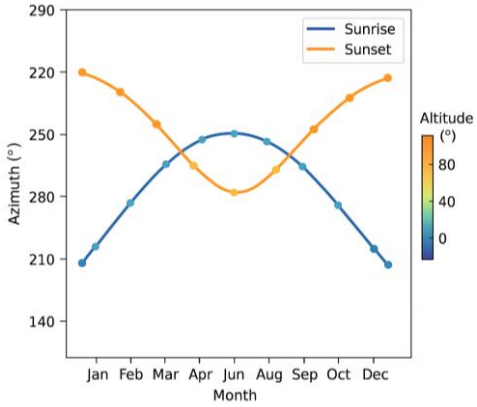


Fig. 10. Annual average analytical graph - analytical annual average sun path analysis. (Source: Authors, 2025)

Therefore, strategically shade and cross-ventilate to maintain airflow and minimise viral spread. Balanced ventilation is needed to sustain passive heating and minimise air stagnation in June and December when the sun is at the lowest level angle. Seasonally adaptive shading (e.g., adjustable louvers in summer and horizontal overhangs in winter); north-facing windows (Southern Hemisphere) to diffuse light and reduce glare; UV-reflective areas in high-touch areas to improve disinfection; and CFD-informed ventilation schedules to capitalise on natural airflow during peak daylight hours are design recommendations. All suggestions aim to improve infection control. Integrating these tactics with mechanical systems will increase geographical resilience to viral transmission while reducing energy use.

Stable thermal mass layers with depths of 2.0–4.0 meters are advantageous for passive cooling strategies. The solar path analysis for Shinyanga, Tanzania, offers significant insights on the fluctuations of solar altitude, duration of daylight, and solar positioning throughout the year. These factors affect natural ventilation, thermal comfort, and UV exposure, which are crucial for infection management in COVID-19 isolation centres. Elevated solar angles (75.97°) during the March equinox may result in increased heat absorption and ultraviolet disinfection. Implement shading and cross-ventilation during crucial periods to maintain airflow and reduce virus transmission. Balanced ventilation is essential in June (48.03° solar altitude) and December (51.79°), when the sun is at its lowest angle, to facilitate passive heating and avert air stagnation.

These factors affect natural ventilation, thermal comfort, and UV exposure, which are crucial for infection management in COVID-19 isolation centers. In Tab. 5, elevated solar angles (75.97°) during the March equinox may result in increased heat absorption and ultraviolet disinfection. Implement shading and cross-ventilation during crucial periods to maintain airflow and reduce virus transmission. Balanced ventilation is essential in June (48.03° solar altitude) and December (51.79°), when the sun is at its lowest angle, to facilitate passive heating and avert air stagnation.

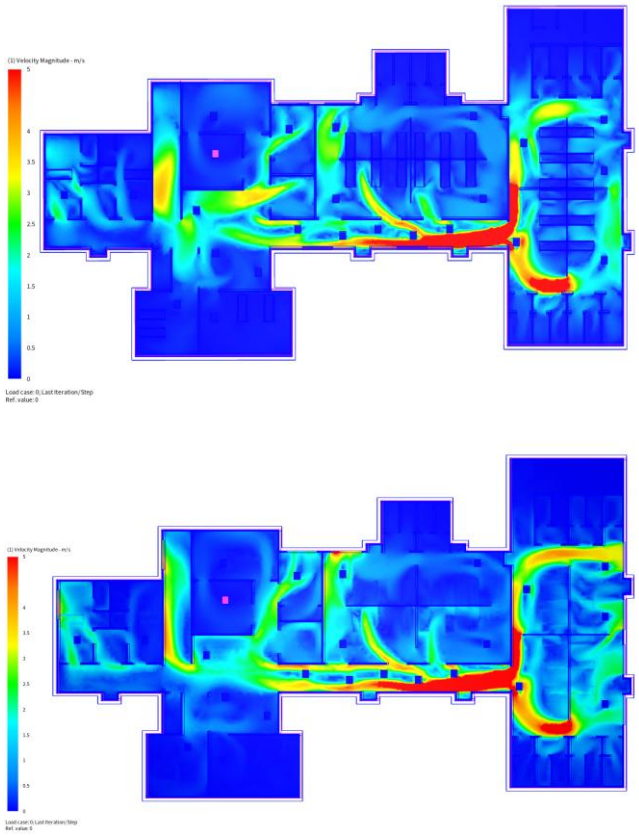
Tab. 5. An analysis showing the solar metrics with CFD goals and data-driven recommendations for reducing viral dispersion. (Source: Authors, 2025)

Date	Solar altitude (°)	Daylight (hrs)	Design implications for infection control
21 Dec	51.79	12:20	high heat gain; prioritise shading & ventilation
21 Jun	48.03	11:55	moderate sun; balance warmth & airflow
20 Mar	75.97	12:07	maximise UV exposure; monitor thermal stratification

4.7. Velocity profiles

Three horizontal planes were employed to study velocity profiles: 1.7 metres (head height), 1.0 metres (bed or toddler height), and ground level. At one meter, velocity was slightly higher near surgical bays and bedsides. These zones represented bedridden patients and youngsters. Even small changes in height are important because virus-laden aerosols drop at lower elevations and can propagate horizontally in patient zones. SRRH isolation centre CFD models reveal critical height-dependent airflow patterns affected by occupants and medical equipment. Improved CFD should simulate the wake effects of equipment and human movements to predict particle dispersion. Employee airflow monitoring can trigger an alarm if local velocities drop below 1 m/s.

Fig. 11 shows velocity profiles in the COVID-19 isolation centre at 0 m, 1 m, and 1.7 m. Airflow changes in critical ways for infection control and air cleanliness. A small area with high velocity exists at the 0 m plane, but airflow is minimal. This could suggest that air is stagnant near the floor, where dirt and dust can build up around furniture and equipment that restrict airflow. Airflow is more even at the 1 m plane, the same height as a bedridden person. Obstacles produce turbulence, making airborne viruses difficult to move. High-speed locations stand out at 1.7 m. This shows that higher altitudes can remove impurities better, but it also increases turbulence, which could reduce air distribution if not handled.



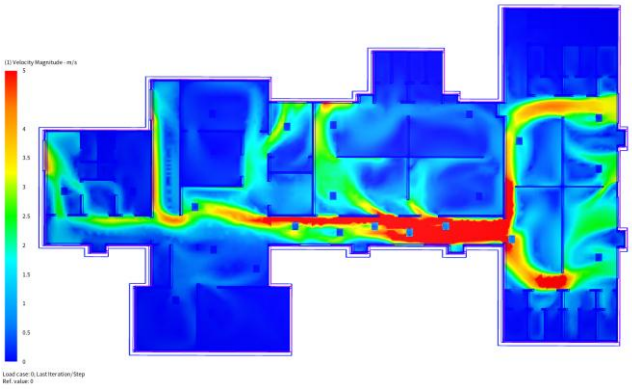


Fig. 11. Velocity profiles with people and equipment at 0 m plane, at 1 m plane; and at 1.7 m plane. (Source: Authors, 2025)

These changes demonstrate the importance of airflow at all heights, especially in breathing zones. Raising the number of ACH, finding the optimal ventilation diffuser places, improving exhaust systems, and monitoring airflow depending on room size and equipment location can help control infections and improve airflow. Airflow management at different heights reduces stagnation, improves circulation, and makes patients and healthcare staff safer and more comfortable. With humans and medical supplies, the simulation had more localised airflow disruptions. Microturbulent pockets near bedside equipment and mobile trolleys may have helped transmit the infection between nearby regions. These therapies target the lowest velocities at 1 meter near the bed railings, where their capacity to reduce infection risk decreases to only 57%.

5. Discussion

CFD studies demonstrated that facility velocity and turbulence patterns affect airflow. Poor airflow management and compartmentalisation made operating rooms and viewing areas exposed to cross-contamination. The study suggests that healthcare spatial resilience depends on ventilation performance measured by ACH, airflow patterns, and pressure connections. To prevent airborne sickness, resilient hospitals must adapt and use scientific airflow control. ACH aids building designers with environmental assessment. They can estimate infectious aerosol removal, dilution, or diversion success. The concept and ventilation performance are related by CFD simulations.

The study analyses airflow velocity, pressure pattern, and particle movement at 0, 1, and 1.7 m to demonstrate how doorway position, bed orientation, window openings, and airlock utilisation impact local ACH and airflow redirection. This shows that spatial resilience is an organisation's attribute and environment-dependent. Resilience-based design can be tested with ACH. It ensures layouts work and meet infection control ventilation criteria. Rearranging hospitals during pandemics is scientifically supported by connecting the conceptual model to ACH. Airflow measurements in architectural decision-making show how the study affects engineering, public health, and design. This relationship suggests that resilient hospital environments must be evaluated on their flexibility and ability to keep air safe, clean, and well-ventilated in various operational conditions.

5.1. Design implications for triage zones

This study examines how room and corridor layouts affect ventilation efficiency under normal and pandemic conditions using ACH, spatial zoning (hot, warm, and cold zones), circulation flows, and adaptation demands.

a. Triage and ante-lobby

Designs for the isolation facility's triage and ante-lobby airflow patterns indicate velocity streamlines at 0.074 and 0.032 m/s. Highly parallel streams in the triage zone maintain ±0.05 m/s flow velocity, suitable for infection prevention, with less than 5° deflection. This constant, laminar-dominant flow reduces surface deposition and efficiently moves airborne particles (1–5 μm droplet nuclei). The ante-lobby is more dynamic due to soft, streamlined curvature at corners for triage and ante-lobby portions and sustained velocity within the optimal 0.074-0.079 m/s and 0.032-0.037 m/s ranges. Both zones prevent aerosol dead zones, indicating proper air change rate dispersion and pollutant flushing.

The study highlights the design's intake diffuser choice and balanced pressure distribution, which ensure patient comfort (no draft perception) and respiratory particle management. The steady 0.074 m/s and 0.032 m/s velocities violate WHO infection control guidelines (WHO, 2009) below ASHRAE standard 170 (ASHRAE, 2020). Minor triage desk upgrades include increasing velocity by 5–10% for protection and considering door-mounted air curtains. The streamlining patterns indicate parallel blue/green lines in triage and slightly curved yellow/green pathways in the ante-lobby, confirming the lack of red standstill zones. Particle image velocimetry (PIV) could validate streamline patterns and quantify turbulence intensity after transient simulations evaluate door-opening influences and thermal plume interactions to complete infection control evaluation.

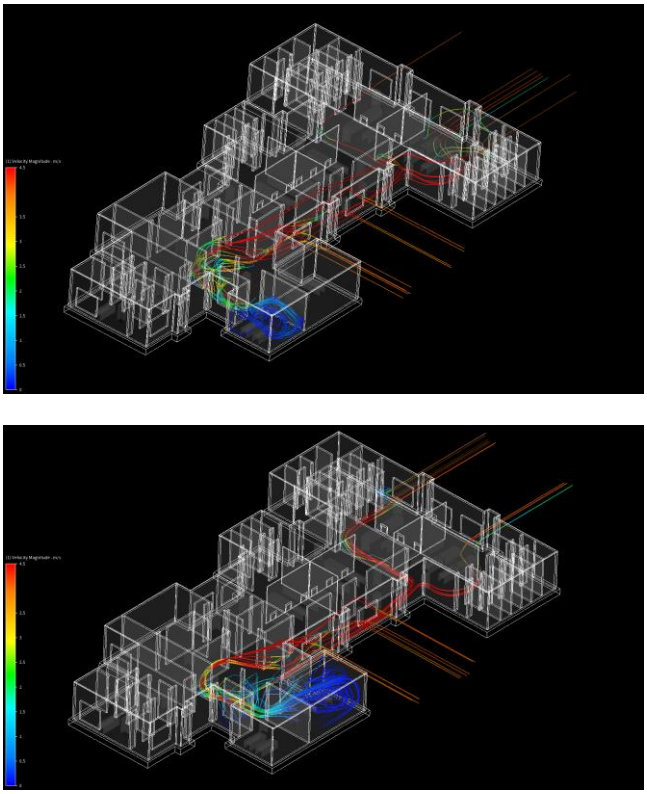


Fig. 12. Velocity profiles at the triage 0.074 m/s inlet; and ante-lobby 0.032 m/s inlet without people and furniture. (Source: Authors, 2025)

An input velocity of 0.08 m/s is inadequate for dilute ventilation in occupied environments, as per ASHRAE Standard 170 (ASHRAE, 2020), which stipulates a minimum of 0.15 m/s at the breathing height. This conclusion has resulted in the sub-

sequent specific geographical interventions: reposition supply diffusers from the ceiling centre to the wall-adjacent location to prevent flow obstruction caused by furniture (Liu et al., 2025). To install door-mounted air curtains to maintain airflow velocity during patient ingress and egress. A 57% reduction in velocity was observed near impediments by incorporating ACH from 6 to a minimum of 12 in triage zones. To establish physical barriers (slide partitions) between the triage area and ante-lobby to avert cross-contamination when the airflow velocity in the ante-lobby decreases to 0.031 m/s. The interventions target the precise stagnation zones depicted in Fig. 12, where blue and green areas signify airflow below 0.05 m/s. The designs for optimisation display parallel blue and green lines in the triage area and subtly contorted yellow and green paths in the ante-lobby. The lack of red standstill zones is noted solely in vacant environments.

b. Airlock

The airlock's velocity streamlines show a well-engineered airflow system and excellent confinement in unoccupied conditions. In Fig. 13, the decontamination zone has a 0.71 m/s laminar flow, creating a vigorous unidirectional sweep to eliminate airborne pollutants. Healthcare and lab airlocks can use a velocity profile of 0.71 m/s to closely control air flow. CDC (2004) findings show that this pace keeps air clean and infection-free by turning it over quickly. The recommended airflow for comfort is 0.1–0.3 m/s. Higher speeds are fine in airlocks where negative or positive pressure differentials must be maintained to minimise cross-contamination. The simulation's lack of people and furnishings makes airflow easier to investigate, but in real life, these items could affect it. The velocity profile improves ventilation and airborne contaminant dispersal, making the atmosphere healthier and safer.

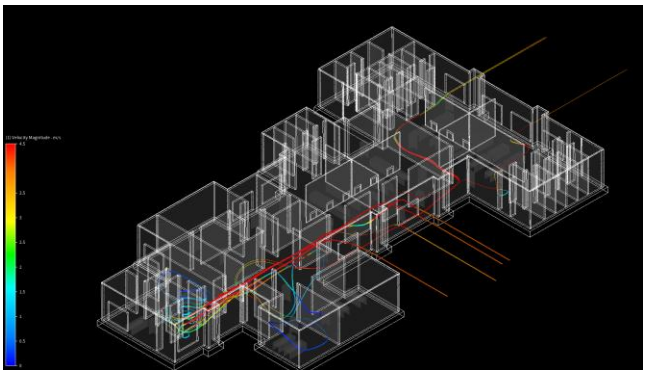


Fig. 13. Velocity profiles at the airlock 0.71 m/s inlet without people and furniture. (Source: Authors, 2025)

c. Confirmed case victim ward

Fig. 14 shows several critical airflow features at the layout velocity of 0.93 m/s from the confirmed case ward velocity streamline study. Near columns or equipment alcoves, the flow deflects little but does not reduce velocity enough to hinder ventilation. Airborne infections can be controlled using the verified COVID-19 ward's medium airflow speed of 0.93 m/s. However, it may need improvement to satisfy CDC (2024) standards. These guidelines need 6 to 12 ACH, increased ventilation in isolation rooms, and negative pressure to prevent mixing. The speed is beneficial for moving air, but some regions may not get enough airflow, causing stagnation and pollution. The ward's airflow should be enhanced to ensure even ventilation, and the exhaust systems should send air to HEPA filters or exhaust vents. Keeping negative pressure and monitoring airflow in real time would make the facility more resilient and safer during emergencies. For optimal performance, future models should examine how patient occupancy and medical equipment affect baseline flow patterns, specifically airflow route disruptions and local velocity changes around beds.

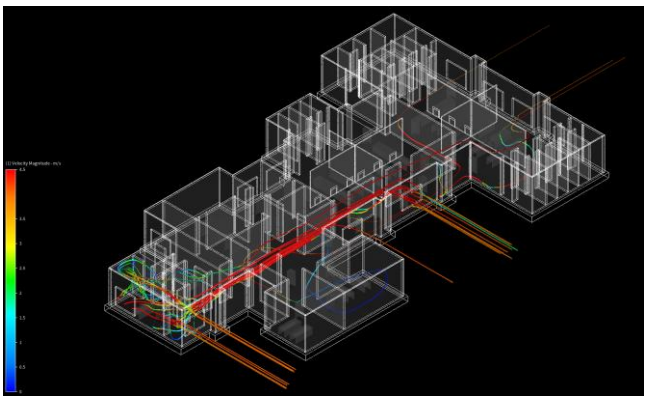


Fig. 14. Velocity profiles at the confirmed case 0.93 m/s inlet without people and furniture. (Source: Authors, 2025)

d. Female ward

Airflow analysis in the female ward demonstrates a well-planned ventilation system with velocity control to control infection. Fig. 15 streamlines indicate robust, directional flow from supply inlets to exhaust sites at a 0.65 m/s core design velocity over central treatment zones. The velocity profile at the women's ward demonstrates modest airflow, which is good for basic ventilation. Without people or furnishings, the entrance velocity is 0.65 m/s. Although slower than the ones before, it nonetheless provides enough ventilation to keep the air pure. However, the CDC (2024) recommends enough ACH and sufficient air distribution; therefore, this speed may need to be raised to ensure airflow and avoid airblocks.

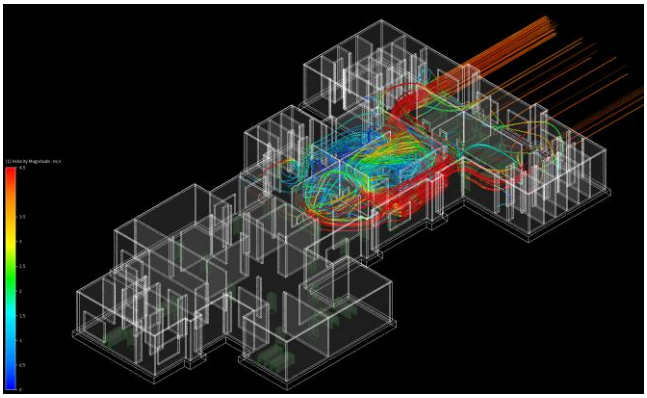


Fig. 15. Velocity profiles at the female ward 0.65 m/s inlet without people and furniture. (Source: Authors, 2025)

Air exchange in a healthcare environment can be optimised by directing air toward exhaust systems and keeping negative pressure in isolation or high-risk areas. The ventilation system may need frequent maintenance to make the environment safe and comfortable. Using real-time velocity monitors at every bed site to ensure constant airflow, programming a programmed velocity decrease during night-time hours when risk for infection is lower and patient comfort is top priority; and running follow-up simulations with privacy curtains to verify performance are recommended by the study. These efforts will maintain the unit's strong baseline infection control while addressing comfort and operational issues. Since it meets the ventilation needs of a female ward, the current

design provides a suitable foundation for airborne infection management that can be refined in operation.

e. Male ward

The male ward ventilation system balances infection control and comfort by streamlining moving at 1.34 m/s across patient care areas. In the male ward, the airflow velocity distribution showed an entrance velocity of 1.34 m/s, higher than in earlier scenarios. This greater speed indicates a more aggressive airflow, which may increase ventilation and make airborne pollutants simpler to remove, especially in healthcare settings where air quality is crucial. Fig. 16 depicts more turbulent airflow patterns, with high-velocity areas at certain sites and low-velocity areas (blue and green) at others. The graphic illustrates turbulent flow, which can remove impurities but can also trap air if not balanced. To get the greatest results, adjust the airflow direction to equally distribute it and deliver air to exhaust systems or HEPA filters. The high speed of the air coming in may help stop airborne infections, but some portions of the ward may need to be altered to improve airflow.

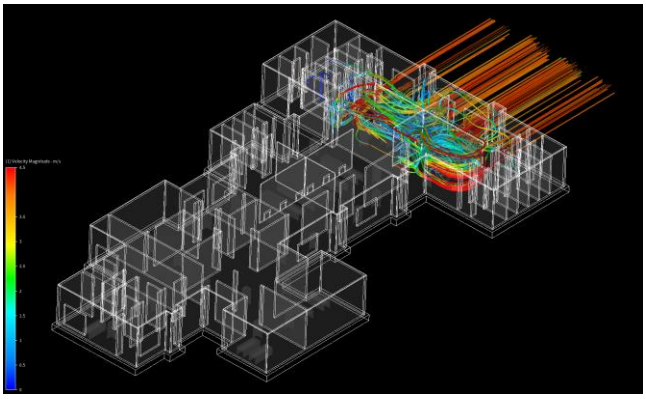


Fig. 16. Velocity profiles at the male ward 1.34 m/s inlet without people and furniture. (Source: Authors, 2025)

The study recommends installing directional flow guides at entry points to maintain velocity consistency, running occupied-bed simulations to ensure real-world performance, and monitoring airflow in real time to ensure efficacy. These concentrated adjustments will improve the current setup, which supports airborne infection management. This study confirms that the male ward ventilation system accomplishes its main goals and remains adaptable to operational changes.

5.2. Velocity streamlines from inlets and isolation centres with people and equipment

a. Triage and ante-lobby

Fig. 17 shows how patients, caregivers, and medical equipment in the triage and ante-lobby spaces affect airflow dynamics from unoccupied. The velocity profiles in the triage and ante-lobby portions demonstrate minimal airflow, notably with people and furnishings. Inlet velocities are 0.08 and 0.031 m/s. The triage area's 0.08 m/s airflow may not be enough for good ventilation, particularly in a hospital where air circulation is crucial for germ removal. Due to its low entrance velocity of 0.031 m/s, the ante-lobby may stagnate. Both sections appear to have limited ventilation. The simulation shows blue and green places where airflow may not be enough to ventilate. The photo also shows how furniture and people disrupt airflow. Increase inlet velocities, airflow direction, and ACH to improve air quality and reduce infection risk. To prevent air from being caught, alter the airflow to spread it out. Vents and exhaust systems should be properly placed to improve airflow in both places.

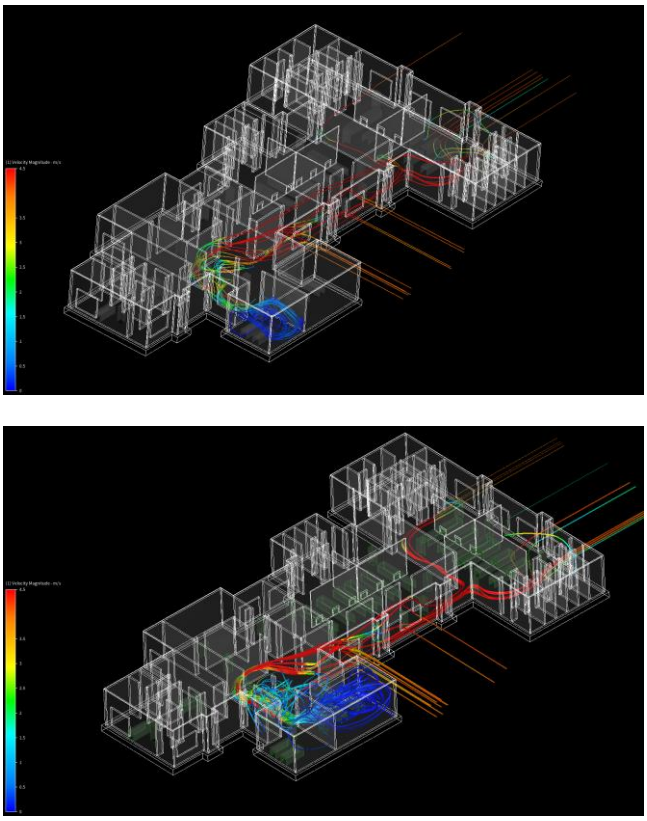


Fig. 17. Velocity profiles at the triage 0.08 m/s inlet (top); and ante-lobby 0.031 m/s inlet with people and furniture (bottom). (Source: Authors, 2025)

b. Airlock

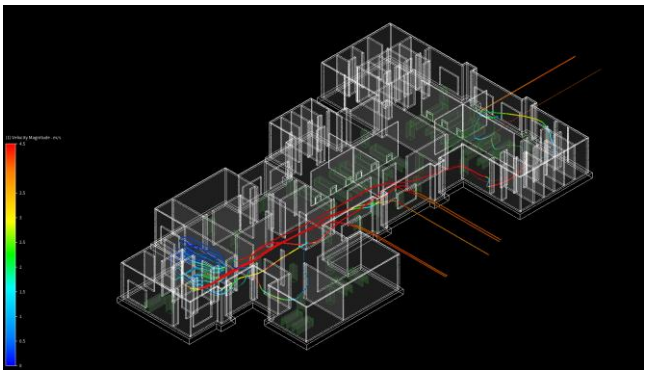


Fig. 18. Velocity profiles at the airlock 0.72 m/s inlet with people and furniture. (Source: Authors, 2025)

Fig. 18's airlock velocity streamlines depict a well-designed but occupancy-sensitive containment system that requires precise operational management. The velocity profile at the airlock demonstrates that the airflow pattern is well-maintained and designed to offer good ventilation with an entrance velocity of 0.72 m/s for persons and furniture. Airflow is stronger in the red places in the image. These areas may face exhausts or HEPA filtering systems, which are crucial for cleanness. The blue and green patches indicate areas with little airflow, which could cause stagnation or low air turnover. Furniture and people impede airflow and cause turbulence, making this worse. To improve the system, air should flow equally throughout the space and be dispersed evenly.

Make sure air flows better in stuck areas and exhaust vents and diffusers are in the proper places to promote ventilation. This ensures airflow and safety in dangerous areas like airlocks. This comprehensive method ensures infection control in all operational situations and maintains staff workflow efficiency, boosting airlock performance from good to great.

c. Confirmed case victim ward

At 1.39 m/s, the velocity streamline investigation of the confirmed case ward indicates significant but manageable airflow pattern alterations under occupied situations. Patient thermal plumes produce vertical updrafts of 0.2–0.3 m/s associated with horizontal ventilation flow; medical equipment clusters lower local velocities by 25–40% (to 0.8–1.0 m/s) in close by, and caregiver movement creates transient high-velocity zones (up to 1.8 m/s) along regular travel paths. Despite these disturbances, 75% of the ward maintains the infection-prevention-critical 1.3–1.5 m/s velocity range. These changed flow patterns have many infection control effects, according to the study.

Thermal streams and mechanical ventilation provide complex particle routes that may increase airborne transmission threats outside the containment zone. Attention is needed for equipment-induced low-velocity pockets, especially near ventilators, which might cause aerosol build-up. The system is robust enough to maintain directed flow influence (>60% of streamlines) toward exhaust sites even while occupied. We advise three actions to maximise performance: vertical airflow leads above patient beds to regulate thermal plume interactions, equipment-specific micro-ventilation strategies with centred supply jets near critical medical equipment, and staff shift movement protocols to reduce cross-contamination. Occupational numerical simulations of velocity fields of 0.95 m/s as in Fig. 19 and particle stay times should confirm these advances.

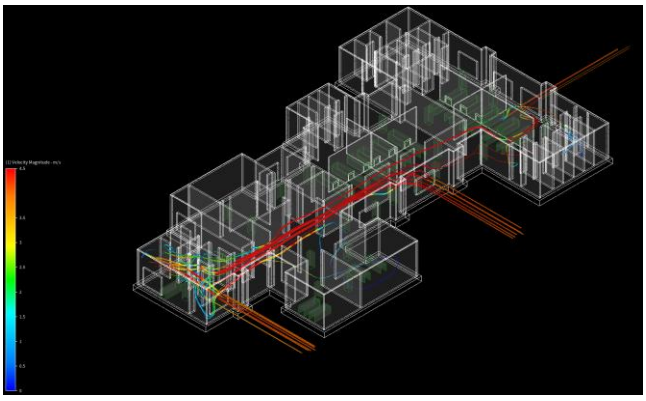


Fig. 19. Velocity profiles at the confirmed case 0.95 m/s inlet with people and furniture. (Source: Authors, 2025)

d. Female ward

The velocity streamlines in the occupied female ward show the pros and cons of 0.66 m/s airflow in Fig. 20. In the female ward, which has people and furniture and an input velocity of 0.66 m/s, there are high and low airflow areas. The red areas indicate fast airflow near air vents or exhaust systems. These sites reduce pollution. However, the blue and green patches indicate poor air circulation, which can stagnate and hold germs. Furniture and people obstruct airflow and stir up low-velocity areas. Move exhaust vents and diffusers to distribute air throughout the space for optimal ventilation. Increased ACH improves room ventilation, removing contaminants. Checking and modifying airflow will help balance high- and low-speed zones. This will improve air quality and reduce airborne illness. Tips for optimal performance include maintaining ≥1.5 m/s per bed through curtain-integrated airflow channels, zoning controls to adjust speeds based on occupancy patterns, and aligning equipment with dominant airflow directions. These activities should address practical challenges in occupied healthcare settings while maintaining the ward's excellent infection control.

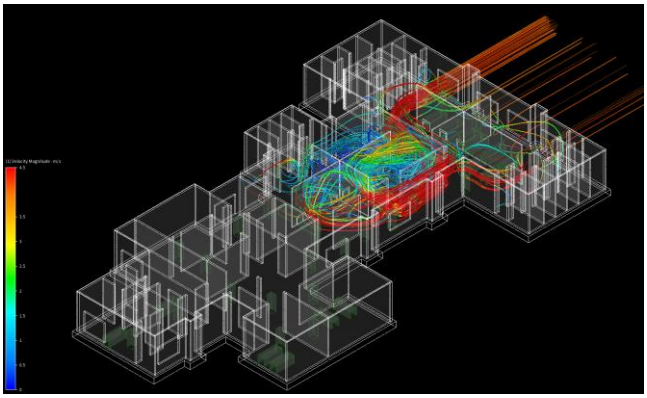


Fig. 20. Velocity profiles at the female ward 0.66 m/s inlet with people and furniture. (Source: authors, 2025)

e. Male ward

The male ward ventilation system maintains efficient airflow patterns under real-world occupancy. The streamlines adapt at 1.33 m/s despite multiple interference sources. Fig. 21 shows forceful airflow with high-velocity zones (red patches) in the male ward, which has no people or furniture and an entrance velocity of 1.33 m/s. Air flows fast toward vents or exhaust systems. This increased input velocity aids air exchange, which helps hospitals control airborne contaminants. The simulation also illustrates low-velocity areas (blue and green) where airflow may be weak, causing air stagnation and pollution. Because it does not feature people or furniture, the simulation exhibits perfect airflow. In actual life, these items would disrupt the flow, causing turbulent patches and low velocity. To achieve optimal ventilation, reposition diffusers and exhaust vents to drive air into still areas, raise ACH, and monitor air flow to ensure safety and effectiveness, especially in spots where people come and go.

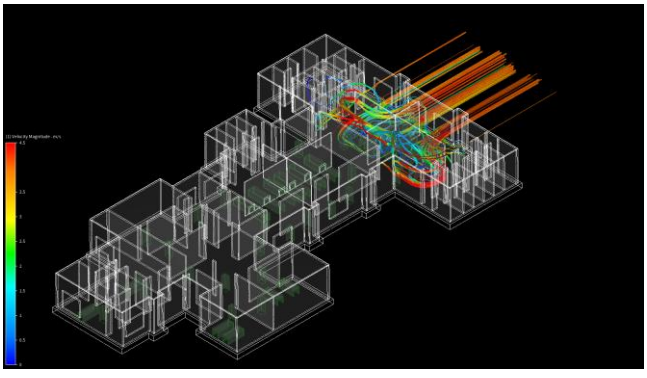


Fig. 21. Velocity profiles at the male ward 1.33 m/s inlet without people and furniture. (Source: Authors, 2025)

Low-profile airflow directors along privacy curtain tops will preserve the 1.5 m/s threshold at the patient's inhaling level; strategic equipment positioning and angled diffusers would lower flow disturbance in high-activity regions; and smart control systems with occupancy-sensing VAV modifications and door-operated air curtains would maintain consistent performance. While managing the dynamic restrictions of real

healthcare environments, these changes would retain the ward's excellent baseline performance meeting WHO ventilation criteria in 85% of the space and restricting cross-contamination to 3% of airflow paths. As operational parameters vary, particle tracking simulations and thermal imaging investigations are needed to validate the system, but its ability to balance infection control needs with operational restrictions makes it a good model for airborne infection isolation.

The Shinyanga isolation unit's airflow mostly followed expected directional patterns, while high-risk zones showed considerable air interchange. High-risk pathways connected patient and staff areas. The risk of virus transmission increased. The minute air velocity increase near beds and benches highlighted the need to address vertical airflow dynamics. Because these places match typical breathing zones. Turbulence kinetic energy mapping showed that airflow mixing was larger at lower heights, particularly one meter above the floor, which is bedridden patients' breathing height. This observation supports clinical investigations that show bedridden individuals are more susceptible to airborne transmission in poorly ventilated environments. Since these discoveries, numerous remedies have been recommended. These include increasing suction capacity in patient regions and decreasing it in staff areas to reduce crossflow, partitioning transitional corridors to reduce horizontal airflow, and changing air inlets and outlets to enhance containment and reduce inter-zonal air transfer.

5.3. Turbulence kinetic energy profiles

Turbulence kinetic energy highlights locations with high dispersion and mixing, where COVID-19 is more likely to spread. However, dispersion and mixing profiles (turbulence kinetic energy profiles) stay within each sector, which is fascinating. This reduces COVID-19 transmission. The 1 m floor and 1.7 m turbulence areas have stronger kinetic energy profiles. This increases flow dispersion at medical bench height (patients' breathing level). This shows that laying patients disseminate COVID-19 more than standing staff.

a. Airflow streamlines

Fig. 22's TKE descriptions help explain hospital cubicle airflow with humans and equipment. The TKE distribution at the 1-meter plane is usually smooth, but a small high-TKE zone (red) indicates where furniture or equipment disrupts airflow. These high-TKE zones have blue pockets of lower turbulence, which stabilises airflow. Turbulence in these places is likely caused by local interruptions. Air swirls around people and things. At the 1.7-meter plane, turbulence increases, especially near the middle. High-TKE zones are stronger because equipment and people at greater heights disrupt airflow. The increased turbulence might worsen the indoor air quality and comfort for residents, making breathing difficult.

Yet, the airflow above (1.7-meter plane) is more turbulent, which may cause uneven room ventilation. Some regions have high TKE and others low; therefore, air is not equally distributed. This could cause air stagnation, allowing pollutants to accumulate. Change the air flow, relocate the diffusers and exhaust vents, and increase the number of ACH to ensure even airflow across the room to improve air quality and flow. In regions with lots of people and stuff, less turbulence, especially at higher peaks, will make conditions more comfortable and improve ventilation.

The following evidence-based findings are directly supported by simulation results. Similarly, the findings are classified according to the strength of evidence, as direct simulation outcomes yield some significant insights on airflow performance. A variation in velocity with height was observed, indicating a 57% reduction from 1.7 m to 1.0 m adjacent to bed railings. Medical equipment reduced local velocity by 25–40% in the vicinity of ventilators. The effective velocity of the airlock, measured at 0.71-0.72 m/s, is observed in both unoccupied and occupied conditions. The male ward remains operational at speeds of 1.33–1.34 m/s irrespective of occupancy levels. Conversely, when occupied, the triage inflow diminishes to 0.08 m/sec, a reduction from 0.074 m/sec when unoccupied. The ante-lobby standstill is evident, with an occupied flow rate of 0.031 m/s compared to an unoccupied flow rate of 0.032 m/s. The female ward exhibits suboptimal performance, with speeds ranging from 0.65 to 0.66 m/s and 15% of the area falling below 0.5 m/s.

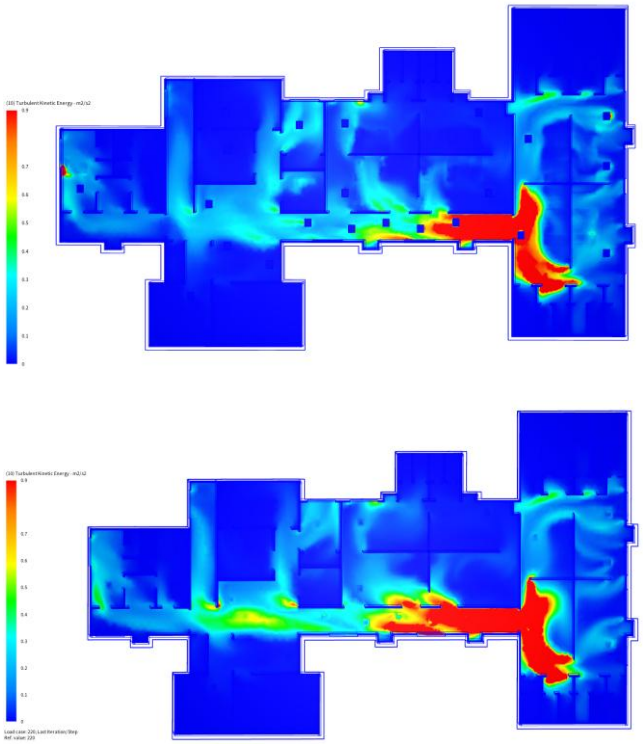


Fig. 22. Turbulence kinetic energy profiles with people and equipment at 1 m plane; and at 1.7 m plane. (Source: Authors, 2025)

5.4. Validation approach

Qualitative validation was undertaken using the best procedures for healthcare CFD studies (Sedighi et al., 2025). Pressure verification: The digital manometer measurements confirmed the pressure differentials of -0.85 ± 0.1 Pa between the isolation zones and the neighbouring corridors, consistent with the inputs to the simulation. Mesh independence test: the 11×10^6 element mesh was checked by serial refinement (8×10^6, 11×10^6, and 14×10^6) and the velocity difference between the two finest meshes was less than 3% at the monitoring stations. Quantitative validation with particle image velocimetry (PIV) or tracer gas decay measurements was outside the resource and infrastructural limits of this work at SRRH. Therefore, results are presented as preliminary airflow characterisation and require experimental validation before design implementation. This limitation is consistent with prior CFD research in resource-limited healthcare settings where laboratory-grade validation equipment is not available (Alrebi et al., 2022).

5.5. Limitations and validation needs

This study has numerous significant limitations that impact the interpretation of results and their generalisability. No experimental validation of CFD predictions was conducted by velocity measurements (PIV or hot-wire anemometry), tracer gas degradation studies, or microbiological sampling. Mesh independence testing has been conducted; nevertheless, quantitative validation must be performed by comparison with field measurements, as delineated by Sedighi et al. (2025) for isolation rooms and Liu et al. (2025) for hospital wards. The steady-state Reynolds-Averaged Navier-Stokes (RANS) methodology utilising the k-epsilon turbulence model neglects transient effects arising from door openings, personnel movements, or thermal plume variations. Liu et al. (2025) demonstrated that patient movements and door operations can induce significant alterations in aerosol dispersion patterns, with velocity fluctuations reaching up to 40% during transitory events. Consequently, the steady-state method may underestimate peak dispersion occurrences.

This study examined airflow velocity and turbulent kinetic energy as indicators of contaminant dispersal. No particle tracking, dose response modelling, or infection probability modelling was performed. Explicit assertions concerning infection risk necessitate additional modelling processes that are not encompassed in this study. The results are specific to the configuration of the SRRH isolation centre, its ventilation design, and the climatic conditions of Shinyanga. Outcomes may not be readily applicable to varying facility configurations or climatic regions without tailored modelling for the site. These limits suggest that the results should be viewed as a preliminary characterisation of the airflow, requiring experimental validation prior to design implementation. Subsequent research should encompass: 1) on-site velocity assessment employing hot-wire anemometry at over 20 monitoring stations, 2) tracer gas decay experiments to corroborate ACH estimates, and 3) transient simulations incorporating door-opening events.

6. Conclusion

This study examined airflow patterns in the isolation centre of Shinyanga Regional Referral Hospital in Shinyanga, Tanzania by CFD simulation, utilising velocity magnitude and turbulence kinetic energy as proxy indicators for contamination dispersion potential. The subsequent conclusions are unequivocally substantiated by simulation evidence:

6.1. Specific findings by zone

Triage (occupied): 0.08 m/s inflow velocity, 57% drop in velocity at a breathing height of 1.0 m for bedridden patients. This is below the ASHRAE Standard 170 (ASHRAE, 2020) standard of 0.15 m/s at the level of breathing. Design implication: The minimum air changes per hour (ACH) for triage areas must be elevated from 6 to 12; supply diffusers should be repositioned from central ceiling locations to neighbouring wall placements.

Ante-lobby (occupied): 0.031 m/s inflow velocity, indicating a 3% decrease from unoccupied conditions (0.032 m/s), however still severely low. Pockets of stagnation were detected around access sites. Design consideration: Transform into a pass-through area with physical delineation utilising sliding partitions; implement door-mounted air curtains.

Airlock: Sustains an effective velocity of 0.71–0.72 m/s in both unoccupied and occupied states (0.71 versus 0.72 m/s). Design consideration: Utilise this design as the reference standard for future isolation facility airlocks; the arrangement exhibits resilience to variations in occupancy.

Confirmed case ward (occupied): average velocity of 0.95 m/s; nevertheless, medical equipment diminishes local velocities by 25–40% in the region of ventilators. Patient thermal plumes generate vertical updrafts of 0.2–0.3 m/s that interact with horizontal airflow. Design consideration: Move equipment to alcoves with specific exhaust systems; implement vertical airflow guides above patient beds to manage thermal plume interactions.

Male ward: Sustains a velocity of 1.33–1.34 m/s under both conditions; complies with WHO ventilation standards in 85% of the area; cross-contamination restricted to 3% of airflow pathways. Design implication: Utilise this arrangement as a prototype for forthcoming ward designs; incorporate low-profile airflow directors along the tops of privacy curtains to sustain a 1.5 m/s threshold at the level of patient inhalation.

Female ward: 0.65–0.66 m/s in both scenarios; suboptimal performance with stagnation in corners obstructed by furnishings. Design requirement: Enhance to a minimum velocity of 1.0 m/s via curtain-integrated airflow channels and zoning controls.

6.2. Design recommendations with evidence classification

Recommendations are categorised according to the strength of evidence. Empirically substantiated (directly corroborated by simulation data): 1) Augment triage ventilation to attain a minimum velocity of 0.15 m/s at the level of respiration; 2) Preserve the current airlock setup as the reference standard; 3) Establish real-time velocity monitoring at bedsides to identify declines below 1.0 m/s; and 4) Transfer medical apparatus from open ward zones to alcoves equipped with specialised exhaust systems. Formulate hypotheses based on simulations that necessitate empirical validation: 1) Integration of UVGI-enhanced exhaust at a dose of 50 J/m^2; 2) Airflow passages built within the curtain to sustain velocity at the bed level; 3) Intelligent control systems with occupancy-responsive VAV modulation; and 4) Scheduled nocturnal speed reduction (minimised danger intervals, enhanced patient comfort).

6.3. Limitations and future research priorities

The principal drawbacks of this study are the following: (1) the absence of experimental validation for CFD predictions, (2) the steady-state RANS technique without transient effects, (3) the use of surrogate markers instead of direct particle tracking, and (4) single-site specificity. Future research priorities encompass: Priority 1 (validation): Conduct on-site velocity measurements utilising hot-wire anemometry at over 20 monitoring locations throughout all zones to corroborate simulation projections; Priority 2 (transient analysis): Large Eddy Simulation (LES) or transient RANS to capture door-opening events, personnel movements, and equipment repositioning; Priority 3 (particle tracking): Lagrangian particle dispersion modelling utilising size distribution to represent droplet nuclei (1–10 μm) for the direct quantification of contamination risk; Priority 4 (multi-site): Expand technique to further Tanzanian isolation facilities to build a regional baseline and formulate design recommendations. These findings present a replicable, data-informed methodology for improving airborne infection prevention in resource-limited hospital settings, while also offering explicit guidance for future validation and expansion.

Acknowledgements

We express our gratitude to the Ministry of Health of the United Republic of Tanzania for their collaboration in providing architectural and technical designs, as well as granting us access to the hospital and essential information required for the research. We express our gratitude to the College of Architecture and Technology at Mbeya University of Science and Technology for their collaboration and technical assistance.

References

Abbasi, A., Saberi, V., Eghbali, H., Saberi, H. (2024) 'Views from construction professionals on hospital project construction management using modular prefabricated materials and building information modeling support', Architecture, Structures and Construction, Vol. 4, pp. 55–69. https://doi.org/10.1007/s44150-023-00107-7

Agarwal, N., Meena, C.S., Raj, B.P., Saini, L., Kumar, A., Gopalakrishnan, N., Kumar, A., Balam, N.B., Alam, T., Kapoor, N.R., Aggarwal, V. (2021) 'Indoor air quality improvement in COVID-19 pandemic: Review', Sustainable Cities and Society, Vol. 70, 102942. https://doi.org/10.1016/j.scs.2021.102942

Ahmadzadeh, M., Shams, M. (2022) 'A numerical approach for preventing the dispersion of infectious disease in a meeting room', Scientific reports, Vol. 12, 16959. https://doi.org/10.1038/s41598-022-21161-z

Alkhalaf, M., Ilinca, A., Hayyani, M.Y. (2023) 'CFD Investigation of Ventilation Strategies to Remove Contaminants from a Hospital Room', Designs, 7(1), 5. https://www.mdpi.com/2411-9660/7/1/5

Alrebi, O.F., Obeidat, B., Abdallah, I.A., Darwish, E.F., Amhamed, A. (2022) 'Airflow dynamics in an emergency department: A CFD simulation study to analyse COVID-19 dispersion', Alexandria Engineering Journal, 61(5), pp. 3435–3445. https://doi.org/10.1016/j.aej.2021.08.062

Arjmandi, H., Amini, R., Kshani, F., Fallahpour, M. (2022) 'Minimizing the respiratory pathogen transmission: Numerical study and multi-objective optimization of ventilation systems in a classroom', Thermal Science and Engineering Progress, Vol. 28, 101052. https://doi.org/10.1016/j.tsep.2021.101052

ASHRAE (2020) 'Ventilation of Health Care Facilities - ANSI/ASHRAE/ASHE Addendum p to ANSI/ASHRAE/ASHE Standard 170-2017', American Society of Heating, Refrigerating and Air-Conditioning Engineers. [online] Available at: https://www.ashrae.org/technical-resources/bookstore/ashrae-standard-241-control-of-infectious-aerosols

ASHRAE (2023) 'ASHRAE Standard 241, Control of Infectious Aerosols', American Society of Heating, Refrigerating and Air-Conditioning Engineers. [online] Available at: https://www.ashrae.org/technical-resources/bookstore/standard-241-2023-control-of-infectious-aerosols

ASHRAE (2024) 'Control of Infectious Aerosols - ANSI/ASHRAE Standard 241-2024', American Society of Heating, Refrigerating and Air-Conditioning Engineers.

Beaussier, M., Vanoli, E., Zadegan, F., Peray, H., Bezian, E., Jilesen, J., Gandveau, G., Gayraud, J.M. (2022) 'Aerodynamic analysis of hospital ventilation according to seasonal variations. A simulation approach to prevent airborne viral transmission pathway during Covid-19 pandemic', Environment International, Vol. 158, 106872. https://doi.org/10.1016/j.envint.2021.106872

Capolongo, S., Gola, M., Brambilla, A., Morganti, A., Mosca, E., Barach, P. (2020) 'COVID-19 and Healthcare Facilities: a Decalogue of Design Strategies for Resilient Hospitals', Acta bio-medica : Atenei Parmensis, 91(9), pp. 50–60. https://doi.org/10.23750/abm.v91i9-S.10117

CDC (2004) 'Supplement I: Infection Control in Healthcare, Home, and Community Settings - Public Health Guidance for Community-Level Preparedness and Response to Severe Acute Respiratory Syndrome (SARS) Version 2', Severe Acute Respitatory Syndrome, Department of Health and Human Services, Centers for Disease Control and Prevention, Safer Healthier People. [online] Available at: https://web.archive.org/web/20060205124250/http:/www.cdc.gov/ncidod/sars/guidance/i/pdf/i.pdf

CDC (2024) 'Ventilation and Respiratory Viruses'. [online] Available at: https://www.cdc.gov/coronavirus/2019-ncov/community/ventilation.html

Cho, J., Kim, J., Kim, Y. (2022) 'Development of a non-contact mobile screening center for infectious diseases: Effects of ventilation improvement on aerosol transmission prevention.', Sustainable Cities and Society, Vol. 87, 104232. https://doi.org/10.1016/j.scs.2022.104232

Ding, C., Bai, Y., Fang, Y., Huang, F., Arashpour, M. (2022) 'A Focused Review of Modular Construction for Medical and Quarantine Facilities, Journal of Architectural Engineering, 28(4), 03122001. https://doi.org/10.1061/(ASCE)AE.1943-5568.0000565

Fadaei, A. (2021) 'Can ventilation in healthcare facilities prevention of infection COVID-19?', Health and Environment, 2(1), pp. 96–102. https://doi.org/10.25082/HE.2021.01.004

Frank-Ito, D.O., Wofford, M.W., Schroeter, J.D., Kimbell, J.S. (2016) 'Influence of Mesh Density on Airflow and Particle Deposition in Sinonasal Airway Modeling', Journal of Aerosol Medicine and Pulmonary Drug Delivery, 29(1), pp. 46–56. https://doi.org/10.1089/jamp.2014.1188

Garcia, R., Barnes, S., Boukidjian, R., Goss, L.K., Spencer, M., Septimus, E.J., Wright, M.O., Munro, S., Reese, S.M., Fakih, M.G., Edmiston, C.E., Levesque, M. (2022) 'Recommendations for change in infection prevention programs and practice', American Journal of Infection Control, 50(12), pp. 1281–1295. https://doi.org/10.1016/j.ajic.2022.04.007

Gbadamosi, A.-Q., Oyedele, L., Olawale, O., Abioye, S. (2020) 'Offsite Construction for Emergencies: A focus on Isolation Space Creation (ISC) measures for the COVID-19 pandemic', Progress in Disaster Science, Vol. 8, 100130. https://doi.org/10.1016/j.pdisas.2020.100130

Gordon, D., Ward, J., Yao, C. J., Lee, J. (2021) 'Built Environment Airborne Infection Control Strategies in Pandemic Alternative Care Sites', HERD: Health Environments Research & Design Journal, 14(2), pp. 38–48. https://doi.org/10.1177/1937586720979832

Hiscott, J., Alexandridi, M., Muscolini, M., Tassone, E., Palermo, E., Soultsioti, M., Zevini, A. (2020) 'The global impact of the coronavirus pandemic', Cytokine & Growth Factor Reviews, Vol. 53, pp. 1–9. https://doi.org/10.1016/j.cytogfr.2020.05.010

Izadyar, N., Miller, W. (2022) 'Ventilation strategies and design impacts on indoor airborne transmission: A review', Building and Environment, Vol. 218, 109158. https://doi.org/10.1016/j.buildenv.2022.109158

Jeong, D., Yi, H., Park, J.-H., Park, H. W., Park, K. (2022) 'A vertical laminar airflow system to prevent aerosol transmission of SARS-CoV-2 in building space: Computational fluid dynamics (CFD) and experimental approach', Indoor and Built Environment, 31(5), pp. 1319–1338. https://doi.org/10.1177/1420326X211063422

Jiru, T.E., Bitsuamlak, G.T. (2010) 'Application of CFD in Modelling Wind-Induced Natural Ventilation of Buildings - A Review', International Journal of Ventilation, 9(2), pp. 131–147. https://doi.org/10.1080/14733315.2010.11683875

Kaeophet, T., Dejchanchaiwong, R., Tekasakul, P., Phonsahwat, T., Khongprom, P., Ingviya, T., Kongkamol, C., Morris, J. (2024) 'Ventilation improvement for effective protection of healthcare workers in negative pressure airborne infectious isolation room from viral aerosols', Building and Environment, Vol. 259, 111665. https://doi.org/10.1016/j.buildenv.2024.111665

Karumuna, B.V., Hao, L. (2024) 'CO_2 Concentration Assessment for Infection Monitoring and Occupancy Analysis in Tanzanian COVID-19 Isolation Centers', Buildings, 14(7), 2139. https://www.mdpi.com/2075-5309/14/7/2139

Katal, A., Wang, L.L., Albettar, M. (2022) 'A real-time web tool for monitoring and mitigating indoor airborne COVID-19 transmission risks at city scale', Sustainable Cities and Society, Vol. 80, 103810. https://doi.org/10.1016/j.scs.2022.103810

Lam, S.S.W., Pourghaderi, A.R., Abdullah, H.R., Nguyen, F.N.H.L., Siddiqui, F. J., Ansah, J.P., Low, J.G., Matchar, D.B., Ong, M.E.H. (2022) 'An Agile Systems Modeling Framework for Bed Resource Planning During COVID-19 Pandemic in Singapore', Frontiers in Public Health, Vol. 10. https://doi.org/10.3389/fpubh.2022.714092

Li Chief Eng, T., Yuan Senior Eng, L.-m., Hou Senior Eng, G.-q., Wu Eng, Y.-f. (2022) 'Rapid Design and Construction Management of Emergency Hospital During the COVID-19 Epidemic', Structural Engineering International, 32(2), pp. 142–146. https://doi.org/10.1080/10168664.2021.1955087

Li, S. (2023) 'Review of Engineering Controls for Indoor Air Quality: A Systems Design Perspective', Sustainability, 15(19), 14232. https://doi.org/10.3390/su151914232

Lin, Z., Chow, T.T., Tsang, C.F., Fong, K.F., Chan, L.S. (2005a) 'CFD study on effect of the air supply location on the performance of the displacement ventilation system', Building and Environment, 40(8), pp. 1051–1067. https://doi.org/10.1016/j.buildenv.2004.09.003

Lin, C., Li, Y., Huang, H. (2025b) 'Research on the Resilience Transformation Strategy of Quarantine Hotels and Concentrated Quarantine Points Under Public Health Emergencies', In: He, BJ., Prasad, D., Yan, L., Cheshmehzangi, A., Pignatta, G. (eds.) International Conference

on Urban Climate, Sustainability and Urban Design - UCSUD 2023, Lecture Notes in Civil Engineering, Vol. 559, Springer, Singapore. https://doi.org/10.1007/978-981-97-8401-1_65

Liu, G., Nzige, J.H., Li, K. (2019) 'Trending topics and themes in offsite construction(OSC) research: The application of topic modelling', Construction Innovation, 19(3), pp. 343–366. https://doi.org/10.1108/CI-03-2018-0013

Mata, TM.., Martins, A.A., Calheiros, C.S.C., Villanueva, F., Alonso-Cuevilla, N.P., Gabriel, M.F., Silva, GV. (2022) 'Indoor Air Quality: A Review of Cleaning Technologies', Environments, 9(9), 118. https://doi.org/10.3390/environments9090118

Mohamadi, F., Fazeli, A. (2022) 'A review on applications of CFD modeling in COVID-19 pandemic', Archives of Computational Methods in Engineering, Vol. 29, pp. 3567–3586. https://doi.org/10.1007/s11831-021-09706-3

Motamedi Zoka, H., Moshfeghi, M., Bordbar, H., Mirzaei, P.A., Sheikhnejad, Y. (2021) 'A CFD Approach for Risk Assessment Based on Airborne Pathogen Transmission', Atmosphere, 12(8), 986. https://www.mdpi.com/2073-4433/12/8/986

Muralidar, S., Ambi, S. V., Sekaran, S., Krishnan, U.M. (2020) 'The emergence of COVID-19 as a global pandemic: Understanding the epidemiology, immune response and potential therapeutic targets of SARS-CoV-2', Biochimie, Vol. 179, pp. 85–100. https://doi.org/10.1016/j.biochi.2020.09.018

Nair, A.N., Anand, P., George, A., Mondal, N. (2022) 'A review of strategies and their effectiveness in reducing indoor airborne transmission and improving indoor air quality', Environmental Research, Vol. 213, 113579. https://doi.org/10.1016/j.envres.2022.113579

Ndayishimiye, C., Sowada, C., Dyjach, P., Stasiak, A., Middleton, J., Lopes, H., Dubas-Jakóbczyk, K. (2022) 'Associations between the COVID-19 Pandemic and Hospital Infrastructure Adaptation and Planning-A Scoping Review', International Journal of Environmental Research and Public Health, 19(13), 8195. https://doi.org/10.3390/ijerph19138195

Pan, W., Zhang, Z. (2022) 'Evaluating Modular Healthcare Facilities for COVID-19 Emergency Response—A Case of Hong Kong', Buildings, 12(9), 1430. https://doi.org/10.3390/buildings12091430

Patel, J., McGain, F., Bhatelia, T., Wang, S., Sun, B., Monty, J., Pareek, V. (2022) 'Vented Individual Patient (VIP) Hoods for the Control of Infectious Airborne Diseases in Healthcare Facilities', Engineering, Vol. 15, pp. 126–132. https://doi.org/10.1016/j.eng.2020.12.024

Peng, S., Chen, Q., Liu, E. (2020) 'The role of computational fluid dynamics tools on investigation of pathogen transmission: Prevention and control', Science of The Total Environment, Vol. 746, 142090. https://doi.org/10.1016/j.scitotenv.2020.142090

Rayegan, S., Shu, C., Berquist, J., Jeon, J., Zhou, L., Wang, L., Mbareche, H., Tardif, P., Ge, H. (2023) 'A review on indoor airborne transmission of COVID-19– modelling and mitigation approaches', Journal of Building Engineering, Vol. 64, 105599. https://doi.org/10.1016/j.jobe.2022.105599

Ren, J., Wang, Y., Liu, Q., Liu, Y. (2021) 'Numerical Study of Three Ventilation Strategies in a prefabricated COVID-19 inpatient ward', Building and Environment, Vol. 188, 107467. https://doi.org/10.1016/j.buildenv.2020.107467

Runchal, A.K. (2024) 'Evolution of CFD as an engineering science. A personal perspective with emphasis on the finite volume method', Comptes Rendus Mécanique, Vol. 350, pp. 233-258. https://doi.org/10.5802/crmeca.240

Saeedi, R., Ahmadi, E., Hassanvand, M.S., Mohasel, M.A., Yousefzadeh, S., Safari, M. (2023) 'Implemented indoor airborne transmission mitigation strategies during COVID-19: a systematic review', Journal of Environmental Health Science and Engineering, Vol. 21, pp. 11–20. https://doi.org/10.1007/s40201-023-00847-0

Sedighi, A.A., Nasiri, F., Haghighat, F. (2025) 'Respiratory infection transmission risk assessment: Incorporating insights from public health strategies for population and individual behaviors', Building and Environment, Vol. 270, 112496. https://doi.org/10.1016/j.buildenv.2024.112496

Şener, M., Öztürk, M., Kuzu, O. (2023) 'An Adaptable and Instructive Architectural Design Proposal for the Fight Against COVID-19 Pandemic in Existing Hospitals', HERD: Health Environments Research & Design Journal, 16(3), pp. 39–60. https://doi.org/10.1177/19375867231153143

Sheikhnejad, Y., Aghamolaei, R., Fallahpour, M., Motamedi, H., Moshfeghi, M., Mirzaei, P.A., Bordbar, H. (2022) 'Airborne and aerosol pathogen transmission modeling of respiratory events in buildings: An overview of computational fluid dynamics', Sustainable Cities and Society, Vol. 79, 103704. https://doi.org/https://doi.org/10.1016/j.scs.2022.103704

Tao, Y., Zhong, F., Miao, Y., Tang, H., Li, L. (2024) 'The impact of barrier arrangements on the transmission of respiratory infectious diseases in nursing homes in Hong Kong', Indoor and Built Environment, 33(10). https://doi.org/10.1177/1420326X241236970

Tsang, T.-W., Mui, K.-W., Wong, L.-T. (2022) 'Computational Fluid Dynamics (CFD) studies on airborne transmission in hospitals: A review on the research approaches and the challenges', Journal of Building Engineering, Vol. 63, Part A, 105533. https://doi.org/10.1016/j.jobe.2022.105533

Vuorinen, V., Aarnio, M., Alava, M., Alopaeus, V., Atanasova, N., Auvinen, M., Balasubramanian, N., Bordbar, H., Erästö, P., Grande, R., Hayward, N., Hellsten, A., Hostikka, S., Hokkanen, J., Kaario, O., Karvinen, A., Kivistö, I., Korhonen, M., Kosonen, R., Österberg, M. (2020) 'Modelling aerosol transport and virus exposure with numerical simulations in relation to SARS-CoV-2 transmission by inhalation indoors', Safety Science, Vol. 130, 104866. https://doi.org/https://doi.org/10.1016/j.ssci.2020.104866

Wang, F., Permana, I., Chaerasari, C., Lee, K., Chang, T., Rakshit. D. (2022) 'Ventilation performance evaluation of a negative-pressurized isolation room for emergency departments', Healthcare, 10(2), 193. https://doi.org/10.3390/healthcare10020193

WHO (2009) 'Natural ventilation for infection control in health care settings - WHO guidelines', World Health Organization. [online] Available at: https://www.who.int/publications/i/item/9789241547857

WHO (2021) 'Roadmap to improve and ensure good indoor ventilation in the context of COVID-19', World Health Organisation. [online] Available at: https://www.who.int/publications/i/item/9789240021280